Title
Post-embryonic growth of the zebrafish retina and the anaphase-promoting complex

Author
Wehman, Ann M

Publication Date
2006

Peer reviewed|Thesis/dissertation

Post-embryonic growth of the zebrafish retina and the anaphase-promoting complex

by

Ann M. Wehman

DISSERTATION

Submitted in partial satisfaction of the requirements for the degree of

DOCTOR OF PHILOSOPHY

in

Genetics

in the

GRADUATE DIVISION

of the

UNIVERSITY OF CALIFORNIA, SAN FRANCISCO

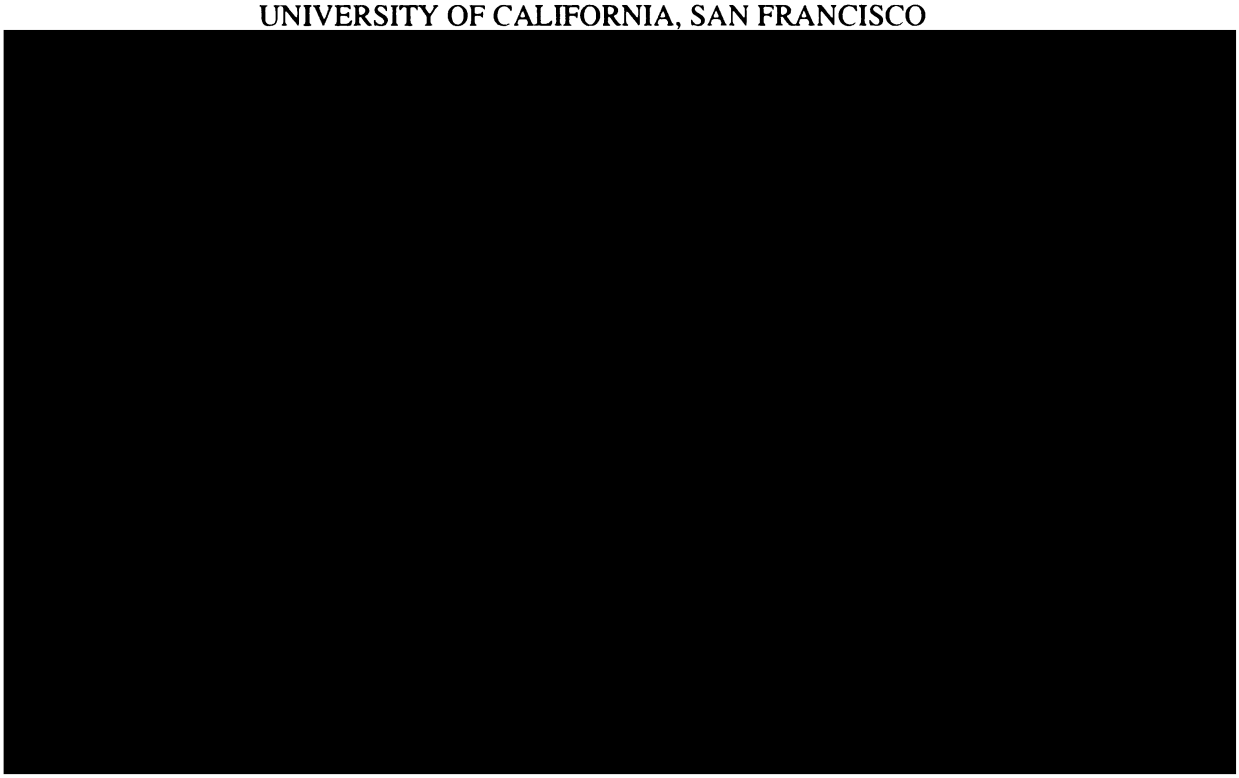

For MM & DD

ACKNOWLEDGEMENTS

I would like to acknowledge my thesis committee: Herwig Baier (chair), Yuh Nung Jan, and Matthias Hebrok. I thank my thesis advisor, Herwig Baier, for his support and for providing me with numerous opportunities to mentor other students. I would also like to thank Didier Stainier for his mentorship. This work would not have been possible without technical assistance from Wendy Staub, Ana Mrejeru, Kerry Deere, Anna Reichardt, and Vicky Kahn. Ellie Heckscher also had a large impact on my graduate career, especially on my writing and presentation style as well as critical thinking.

The cover on page 5 was published in the May 1, 2005 issue of *Developmental Biology* and I produced the photo. The text of Chapter 1 is largely a reprint of the material as it appears in *Developmental Biology* Vol. 281(1) pages 53-65 (2005). The cover and text are reprinted with permission from Elsevier, Inc. The co-authors made the following contributions: Wendy Staub provided vital assistance with cryosectioning and Nissl staining. Jason Meyers analyzed the *s545/she* mutant and assisted with plastic sectioning and methylene blue staining. Pamela Raymond directed and supervised Jason Meyer's work. Herwig Baier directed and supervised the research that forms the basis for this chapter.

ABSTRACT

Post-embryonic growth of the zebrafish retina and the anaphase-promoting complex

Ann M. Wehman

Stem cells divide to create new cells for growth and regeneration throughout the life of an organism. This requires that some stem cells survive through embryonic stages to function in the adult body. Despite the celebrated therapeutic potential of stem cells, the mechanisms used by the body to regulate stem cell proliferation and quiescence are poorly understood.

We performed a forward-genetic screen in zebrafish to discover genes that regulate the division of stem cells specifically in the larval retina. The zebrafish retina is a fantastic system in which to study how stem cells survive embryogenesis and maintain their population at larval and adult stages. The stem cells and their progenitor daughters are found in a stereotyped location at the retinal periphery in a region called the ciliary marginal zone (CMZ) in larvae and adults. In our screen, we discovered mutants where the retina underwent normal development during embryogenesis, but failed to grow normally at larval stages. These mutants fell into two classes, one with a reduced number of cells in the CMZ, and the second with an increased number of cells in the CMZ. We placed these mutants into a hierarchy and propose a model for retinal growth from the CMZ.

We went on to identify the genes responsible for the reduced number of cells in the CMZ in two mutants. We discovered that Cdc16 and Cdc26, two subunits of the anaphase-promoting complex / cyclosome (APC/C), are required for the mitotic division of retinal progenitors in the CMZ. Defects in mitotic progression were also observed in tissues beyond the retina and we additionally found that quiescent cells erroneously re-enter the cell cycle in the absence of Cdc16 or Cdc26. In addition, we discovered that these proteins are stable and wild-type protein derived from maternally-deposited RNA or protein is still functional at late larval stages in mutant animals. These maternal proteins mask the severity of defects caused by loss of the APC/C.

TABLE OF CONTENTS

LIST OF TABLES

CHAPTER 1

CHAPTER 2

LIST OF ILLUSTRATIONS

CHAPTER 1

CHAPTER 2

INTRODUCTION

Stem cells are famous for their ability to make an asymmetric choice. They can divide to produce stem cells and renew their population. They can also divide to create progenitor daughters that undergo multiple amplifying divisions before differentiating. In this way, a single stem cell division can give rise to many cells in a given tissue. The vital role of stem cells in growth and regeneration has made them an obvious target for medical research. The therapeutic potential of a cell that can both survive for long periods of time as well as repopulate a damaged tissue is substantial.

As yet, the therapeutic potential of stem cells for most diseases is largely unproven. This is due in part to large gaps in our knowledge about the biology of stem cells. The inductive forces (such as growth factors) that can act on a stem cell to direct it to differentiate into a particular type of cell have been established for only a small fraction of cell types. Without the ability to control stem cells (or the knowledge of where to place stem cells to allow the proper control), there are dangers associated with stem cell therapy. It is thought that cancer may be the result of unchecked stem cell division. Given this potential complication of stem cell therapies, it is important to understand the mechanisms used by the body to regulate proliferation and quiescence in stem cells.

One example of the fine regulation of stem cells is the existence of adult stem cells. Adult stem cells must maintain their population through the extensive waves of differentiation during embryogenesis whereas embryonic stem cells are used up. The loss of adult stem cells is thought to be one of the causes of the various defects associated

with old age, such as thin skin and poor wound healing. It is unclear how some stem cells survive embryogenesis and maintain their populations for long term.

In order to better understand how stem cells are maintained, we chose to study a population of post-embryonic stem cells in the zebrafish eye. These stem cells are located at the peripheral edge of the retina in a region called the ciliary marginal zone (CMZ) that skirts the lens. The stem cells of the CMZ are responsible for most of the considerable growth of the retina that occurs between 60 hours post-fertilization and adulthood. Stem cells near the lens divide to give rise to rapidly dividing progenitors that amplify each stem cell division to eventually produce many neurons and glia. In this manner, new cells are constantly being added to the margins of the retina and the central retina is made up of the oldest cells, the ones that differentiated during embryogenesis. Given the stereotyped layout of stem cells, progenitors, newly differentiated cells, and older differentiated cells in the zebrafish retina, we could overcome a lack of definitive markers for retinal stem cells. Using zebrafish as a model system also gave us advantages in terms of their fast generation time, large number of progeny, and established genetic resources.

In order to discover genes necessary to regulate the division of stem cells and progenitors in the CMZ, we performed a forward-genetic screen. We used a two-tiered approach where we first screened for fish with abnormal growth of the retina (i.e. small eyes at a larval stage) and then examined the morphology of the eye, especially the CMZ. This strategy was very successful and we discovered two classes of mutants that affected post-embryonic growth of the retina. The first class had a dramatically reduced number of cells in the CMZ and fewer dividing cells in the retinal margin, but a normal central retina. The second class had an increased number of cells in the CMZ and also had fewer

successfully dividing cells at the margin. We placed these genes into a hierarchy where the Class I genes were more likely to act in the retinal stem cells themselves or in their immediate progenitor daughters. Class II genes, in contrast, were more likely to act in later progenitors or cells that were preparing to differentiate. This work is described in Chapter 1 and was published in the journal *Developmental Biology* in May 2005.

Having isolated mutants with aberrant proliferation of stem cells or their progenitor daughters, we then went on to identify the genes mutated in these mutants. We discovered that two of the Class I mutants carry mutations in two subunits of the anaphase-promoting complex/cyclosome (APC/C). The APC/C is a complex of at least thirteen proteins that function together as an E3 ubiquitin ligase to target specific proteins for degradation. The APC/C has many targets and regulates multiple steps in the cell cycle, namely the metaphase-to-anaphase transition, mitotic exit, and the length of G_1. In our APC/C mutants, we observed defects consistent with a mitotic arrest in the CMZ as well as in other dividing tissues of the zebrafish larvae. We also observed cells losing the ability to maintain G_0 and re-entering the cell cycle, consistent with the role of the APC/C in regulating G_1. These results confirmed previous findings from other species on the role of the APC/C in regulating the cell cycle. This work is described in Chapter 2.

One surprising facet of the zebrafish APC/C mutant phenotype is how it appears to be restricted to larval stages. The APC/C is expected to regulate every meiosis and mitosis as well as maintaining quiescence. We believe the larval onset is due to maternal protein that rescues the embryonic divisions. In zebrafish, the oocyte is heavily deposited with RNA and protein that regulates at least the first 10 divisions and early patterning. In the case of unstable proteins, such as Cyclin B1 (a degraded target of the APC/C), it is

known that maternal RNA and protein are cleared in roughly one day. We find that our APC/C proteins are stable, first start to be cleared after 2-3 days, and persist for at least a week. We also show that inhibition of the APC/C at early cleavage stages results in defects in division, further substantiating the maternal rescue hypothesis. This work is also described in Chapter 2.

This dissertation details the initial work isolating and characterizing mutants that affect post-embryonic development of the zebrafish retina. Although, we discovered that the APC/C regulates the division of retinal progenitors, it is also likely to regulate every other cell division in zebrafish. The research reported here supports the idea that post-embryonic stem cells simply recapitulate embryonic development. Other researchers at UCSF and beyond are studying the mutants isolated in our screen. Their work will also address whether there exist genes that specifically regulate post-embryonic stem cells or whether maternal rescue of embryogenesis is responsible for the larval onset of phenotypes. In combination with the work described in this dissertation, their research will contribute to our better understanding of the mechanisms used to regulate stem cell division and quiescence.

CHAPTER 1

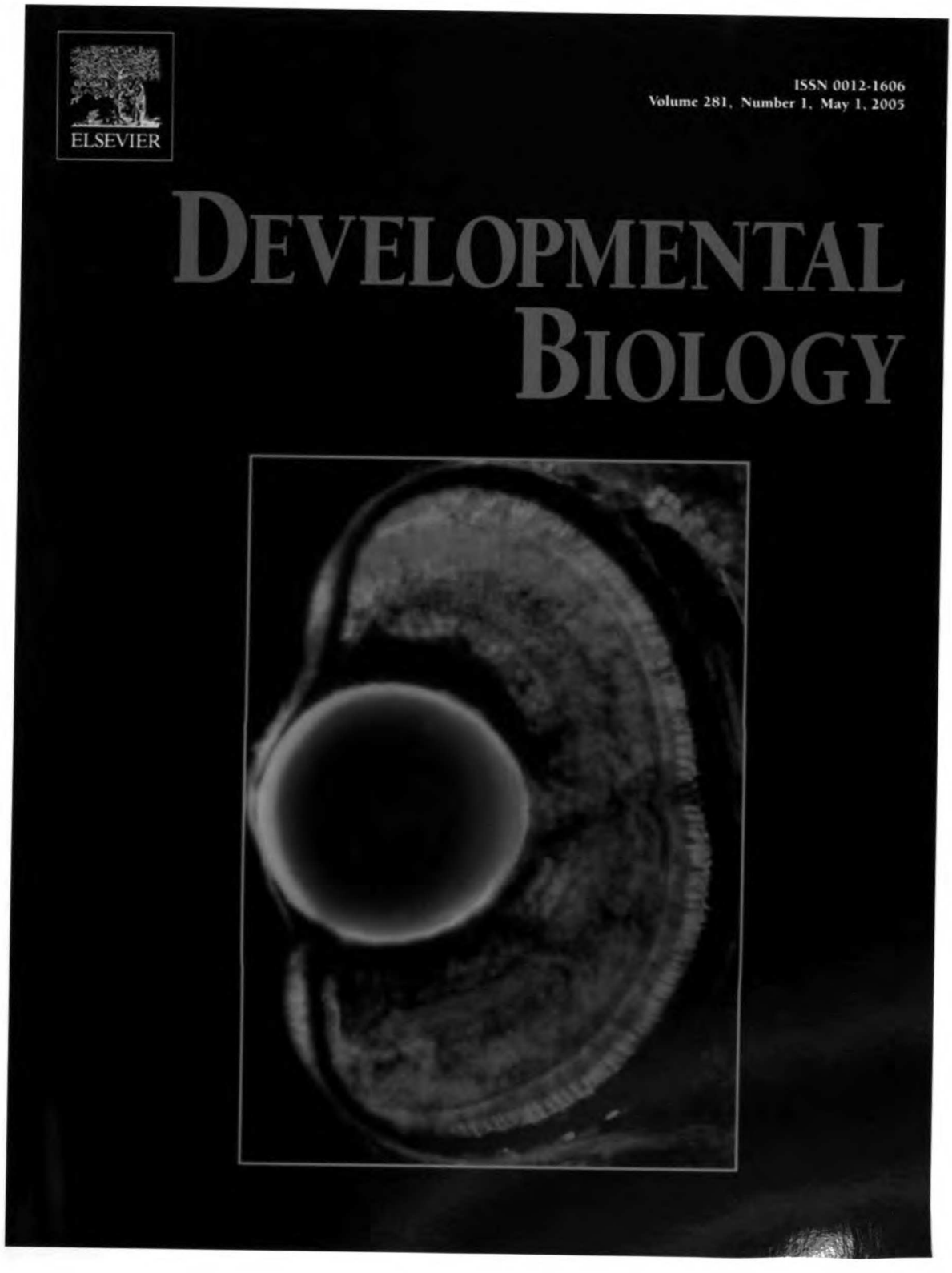

CHAPTER 1

Genetic dissection of the zebrafish retinal stem cell compartment

Ann M. Wehman, Wendy Staub, Jason Meyers, Pamela A. Raymond, and Herwig Baier

SUMMARY

In a large-scale forward-genetic screen, we discovered that a limited number of genes are required for the regulation of retinal stem cells after embryogenesis in zebrafish. In 18 mutants out of almost 2,000 F2 families screened, the eye undergoes normal embryonic development, but fails to continue growth from the ciliary marginal zone (CMZ), the post-embryonic stem cell niche. Class I-A mutants (5 loci) display lower amounts of proliferation in the CMZ, while nearly all cells in the retina appear differentiated. Class I-B mutants (2 loci) have a reduced CMZ with a concomitant expansion in the retinal pigmented epithelium (RPE), suggesting a common post-embryonic stem cell is the source for these neighboring cell types. Class II encompasses three distinct types of mutants (11 loci) with expanded CMZ, in which the progenitor population is arrested in the cell cycle. We also show that in at least one combination the reduced CMZ phenotype is genetically epistatic to the expanded CMZ phenotype, suggesting that Class I genes are more likely to affect the stem cells and Class II the progenitor cells. Finally, a comparative mapping analysis demonstrates that the new genes isolated do not correspond to genes previously implicated in stem-cell regulation. Our study suggests that embryonic and post-embryonic stem cells utilize separable genetic programs in the zebrafish retina.

INTRODUCTION

Stem cells are undifferentiated cells with the capacity to self-renew and to give rise to differentiated daughter cells (reviewed in Cogle et al., 2003). Stem cells often produce a series of short-term rapidly dividing progenitor cells that amplify a single stem cell division to produce many differentiated cells. Embryonic stem cells are totipotent and responsible for the original formation of all tissues in the body during embryogenesis. Post-embryonic stem cells, on the other hand, are more limited in the types of cells they can produce. They reside in specialized niches throughout the body, and are responsible for continuing growth and replenishing lost or damaged cells. The stem cell niche has an important role in maintaining the stem cell population through and after embryogenesis (reviewed in Fuchs et al., 2004).

It is still unclear what signals regulate stem cell maintenance and what cell-intrinsic properties a stem cell must possess to self-renew and maintain multipotency. Several groups have profiled the molecular differences between embryonic and post-embryonic stem cells (Ivanova et al., 2002; Ramalho-Santos et al., 2002; Stappenbeck et al., 2003; Tumbar et al., 2004), but these studies have not identified which genetic programs are important for the maintenance of post-embryonic stem cells. A phenotype-based forward-genetic approach has been applied to the *Drosophila* germline (Lin and Spradling, 1997), an amenable stem cell population because of its stereotyped location and prolific output. This work discovered a novel gene, Piwi, as well as a new role for the translational repressor Pumilio. Subsequent studies found that germline stem cells communicate with their neighboring niche cells using the Jak/Stat signaling pathway to maintain the stem cell population (Kiger et al., 2001; Tulina and Matunis, 2001). A

genetic screen for regulators of somatic stem cells had not been carried out, partly owing to the fact that these cells are absent in the commonly used genetic model systems, *Drosophila* and *C. elegans*. It is therefore not known whether somatic stem cells utilize mechanisms similar to those discovered in the *Drosophila* germline or whether they employ unique pathways.

In the past ten years, zebrafish has become a favorite model system for forward genetic approaches (Patton and Zon, 2001). The visual system of this species has been the focus of several screens (Easter and Malicki, 2002). The optic primordia are first morphologically distinguishable at the 6-somite stage in zebrafish as bilateral outgrowths from the forebrain (Schmitt and Dowling, 1994). By 24 hours post fertilization (hpf), the optic primordia have divided into two major tissues, the neural retina and the retinal pigmented epithelium (RPE) (Li et al., 2000). The first neurons start to differentiate around 27 hpf and embryogenesis of the retina is complete by 60 hpf. From that point on, cell divisions in the central retina are rare and confined to the rod photoreceptor lineage. After 60 hpf, almost all retinal growth comes from the periphery of the eye, from a proliferative region called the ciliary marginal zone (CMZ) (Marcus et al., 1999).

In fish and frogs, the CMZ (also known as the circumferential germinal zone) is a discrete region composed of a rare population of multipotent stem cells and their rapidly dividing progenitor daughters (reviewed in Harris and Perron, 1998; Hitchcock et al., 2004). Regions corresponding to the CMZ of cold-blooded vertebrates have been recently identified in birds, marsupials, and possibly higher mammals (Ahmad et al., 2000; Kubota et al., 2002; Tropepe et al., 2000). The progenitor cells are aligned in the CMZ in a peripheral-to-central gradient, largely recapitulating the dynamic gene expression

patterns observed during embryonic retinal development (Perron et al., 1998). The least committed progenitors are found peripherally, adjacent to the stem cells. Progressively more central progenitors have an increasingly restricted potential, while still maintaining the characteristic elongated shape of mitotically active, neuroepithelial cells. The most central CMZ cells, finally, have left the cell cycle and are undergoing differentiation into one of the seven neuronal or glial cell types in the neural retina. In this manner, the CMZ adds new cells to the retina in concentric rings for as long as the eye is growing.

The CMZ is a true stem-cell niche, whose stereotyped location and prolific output offer an excellent opportunity for a forward-genetic screen. We report here the discovery of 18 mutants that undergo evidently normal embryonic development of the retina, but fail to continue growth from the CMZ. The mutated genes do not encode previously known regulators of stem cells. Based on our phenotypic analysis, we have placed these novel genes in a genetic pathway underlying retinal growth.

RESULTS

Screen statistics and screening strategy

We screened 5,498 F3 clutches from 1,740 ENU-mutagenized F2 families. Based on the number of crosses per F2 family, we calculated that our screen encompassed 1,688 genomes. Following ENU mutagenesis of 50 adult males, we crossed them repeatedly to *sandy* (*sdy*) females and determined that our treatment had induced 6 new *sdy* mutations in slightly over 2,000 of their F1 progeny. Mutation of *sdy* disrupts tyrosinase and leads to a pigmentation defect that is easy to score (Page-McCaw et al., 2004). From this specific locus test, the mutation rate was calculated to be 0.3% per gene per genome. These numbers predict that our screen did not reach saturation, which is confirmed by the observed allele frequencies (see below).

In order to isolate embryos with defective post-embryonic retinal stem cells, our screen used a "funnel" strategy, designed to weed out non-specific mutants. We hypothesized that disruption of the CMZ should result in small eyes at larval stages, because the CMZ is primarily responsible for retinal growth after 60 hpf. We reasoned that this first-pass screen should enrich for mutants with eye growth defects. However, only a small fraction of small-eyed mutants are expected to be CMZ-specific, since disruptions of housekeeping genes, tissue degeneration, or general developmental delay may all result in this phenotype. In fact, almost every F2 family produced an embryonic-lethal small eye mutant, as reported for earlier screens (Haffter et al., 1996; Malicki et al., 1996; Golling et al., 2002). We therefore selected against embryonic mutants by screening for small-eyed fish at late-larval stages, at 6 days post fertilization (dpf). Still,

approximately 20% of F2 families produced at least one small-eyed mutant at 6 dpf (465 clutches from 345 families). We next selected larvae lacking outward signs of gross necrosis and with eyes at least as large as those of a normal 2 dpf embryo (>150 μm along the nasal-temporal axis). Larvae meeting these criteria (269 small-eyed mutants from 246 families, or 14% of all F2 families) were sectioned and stained (see below) for histological analysis of the eye. Figure 1 shows a wild-type larva (Fig.1A) and a small-eyed larva (Fig. 1B) that met our screening criteria.

Of these, 187 mutants showed gross defects in the lamination or differentiation of the central retina, widespread degeneration, or no apparent morphological defects (except for reduced eye size) and were immediately discarded. We found 64 mutants (3.7%) with clear CMZ phenotypes, of which 46 were not further considered. In 24 of the 46 discarded lines, the CMZ was the normal size, but appeared twisted by invading protrusions of RPE. We reasoned that this phenotype was unlikely to be caused primarily by a CMZ defect, but rather by an RPE defect. In 16 of the 46 discarded lines, we observed either a subtle expansion of the CMZ and a normal central retina or a greatly expanded CMZ, but the embryonic central retina appeared severely affected. In mutants with a subtle expansion, it was unclear whether the retinal cells were packed less tightly, and therefore the CMZ was spread out. Mutants with a large expansion of the CMZ and a poorly developed embryonic retina did not specifically affect the post-embryonic growth of the retina, which was the focus of our screen. Six of the 46 discarded lines had only a subtle reduction in the size of the CMZ. In summary, only 18 mutants (1.0% of all F2 families screened) were considered specific and robust (Table 1).

High-throughput analysis of the zebrafish CMZ

Since there are currently no molecular markers specific for retinal stem cells, we scored the CMZ phenotype using morphological criteria. Previous studies had used methylene blue-stained sections to assess retinal morphology (Fadool et al., 1997; Malicki et al., 1996; Neuhauss et al., 1999; Vihtelic and Hyde, 2002). We developed a three-color fluorescent system that provided additional criteria by which to define cell type and shape. First, we used a fluorescent Nissl stain to highlight the CMZ (Fig. 1C). Rapidly dividing progenitors produce high levels of RNA and therefore stain Nissl-bright. The fluorescent Nissl dye stains the CMZ more strongly than methylene blue. Post-mitotic cell types such as retinal ganglion and amacrine cells also stain distinctly with Nissl, but at a level clearly lower than the progenitor cells of the CMZ. As a counterstain, we used DAPI to observe nuclear morphology and the presence of pyknotic cells (Fig. 1E). Due to our fixation conditions, we could also detect autofluorescence of membrane-rich structures such as the synaptic plexiform layers and the outer segments of photoreceptor cells (Fig. 1D).

This fluorescent method, while fast, simple and robust, revealed many details of retinal architecture and was comparable in resolution to classical methylene-blue staining (Fig. 2), although the latter method is better able to show cellular morphologies at high magnification. In the merged fluorescent image, the central retina shows distinct colors for the different layers of the eye (Fig. 1F). Here the ganglion cells are purple, the inner plexiform layer (IPL) is green, the amacrine cells are purple, the bipolar cells are red, the outer plexiform layer is green, the inner segments of the photoreceptor cells are red, and the outer segments of the photoreceptor cells (POS) are green. In comparison, the

peripheral edge of the retina, where the CMZ resides, is pink. The IPL tapers off as it approaches the CMZ and there are several columns of differentiating cells between the IPL and the CMZ. Similarly, the lengths of the outer segments of the photoreceptor cells become shorter as they approach the CMZ. We employed these layering and coloration criteria to assess the phenotypes of the mutant lines when using these fluorescent sections.

Class I: Mutants with reduced CMZ

The first class of mutants discovered by our screen (Class I) is comprised of eight lines, exhibiting one of two related phenotypes, Class I-A and I-B. Class I-A mutants have a dramatically reduced CMZ and retinal progenitors are largely or completely missing. Based on complementation crosses and chromosomal mapping, the six Class I-A alleles correspond to five genes with nearly identical phenotypes: *gog*, *woo*, *zea*, *vij*, and *yol* (Table 1). In all six mutants, there is no bright Nissl stain at the peripheral edge of the retina after 4 dpf (Fig. 3B, compare to A), and few cells display the undifferentiated neuroepithelial morphology characteristic of the CMZ (Fig. 2B', compare to A'). The IPL and outer segments of the photoreceptor cells appear fully developed all the way to the peripheral edge of the neural retina. Based on staining using a panel of markers for six of the seven major differentiated retinal cell types, the embryonic central retina appears normal in Class I-A mutants (Fig. 3C, D, and data not shown). However, at the peripheral edge of the retina, where the cells are immature in wild-type larvae and normally do not stain with these markers (Fig. 3C), the Class I-A mutants have

morphologically normal, differentiated cells (Fig. 3D and data not shown). This further confirms that the undifferentiated progenitor population is missing from the retina.

To test whether cells continue to divide in the reduced CMZ of Class I-A mutants, we immersed the larvae in a solution of BrdU for 12 hours starting at 3 dpf. BrdU is incorporated into actively dividing cells during S-phase. We then stained the larvae with antibodies against BrdU at 5 dpf, when the reduced size of the mutant eye was easily distinguishable from their wild-type siblings. While wild-type larvae display a large number of dividing cells at the peripheral edge of the retina in and next to the CMZ (Fig. 3E), mutants have very few labeled cells (Fig. 3F). The sparse BrdU-labeling in the mutant retina (Fig. 3F) and the presence of differentiated markers at the peripheral edge of the retina (Fig. 3D) suggest that the majority of the retinal stem cell and progenitor population is missing or mitotically quiescent. In contrast, cell divisions outside the retina appear grossly normal based on robust BrdU labeling in other tissues (Fig. 3F, and data not shown). This suggests that the phenotype of Class I-A mutants is somewhat specific for the retinal stem cell and progenitor population and not simply due to an overall decrease in mitoses. Other stem cell populations in the mutant larvae have not been examined, however, and may also be affected. Five of the six Class I-A mutants develop normal swimming behaviors and appear healthy at larval stages, but none have been observed to begin feeding. This suggests that the mutations must affect tissues beyond the retina, because blind fish have been raised to adulthood (Kay et al., 2001). The underlying cause of lethality is unknown.

Class I-B mutants display a reduced CMZ, similar to Class I-A, but also exhibit an expansion in the peripheral RPE overlying the CMZ (Fig. 2C). Two Class I-B mutants

were isolated, *oui* and *kes* (Table 1). Genetic linkage analysis revealed that one of the mutations, oui^{s312}, is caused by a large inversion on chromosome 13 (Table 2 and data not shown). Similar to Class I-A mutants, there is no bright Nissl staining at the peripheral edge of the retina (Fig. 4B), demonstrating that the progenitor population is reduced. In contrast to Class I-A, the lens often appears trapped inside the eye beneath an expanded RPE in Class I-B mutants (Fig. 4B, D). When we performed BrdU-labeling in Class I-B mutants, we again saw a dramatic reduction in the number of dividing cells at the peripheral edge of the retina (Fig. 4F, compare to 4E), further confirming the absence of retinal progenitors. One potential explanation for this phenotype is that the stem cell progeny that should have produced retinal tissue have instead converted to an RPE fate (see Discussion).

Class I-A and I-B double mutant analysis

Based on their phenotypes, we hypothesized that the reduced CMZ, expanded peripheral RPE Class I-B mutants would affect an earlier, more pluripotent retinal stem cell than the reduced CMZ Class I-A mutants. We therefore predicted that a double mutant animal would exhibit the expanded peripheral RPE phenotype, because the stem cells will make RPE at the expense of neural retina. We chose an exemplary mutant from the expanded CMZ Class I-B, *kes* (Fig. 5B), and the reduced CMZ Class I-A, *gog* (Fig. 5C). We mated *kes* and *gog* to create double heterozygous carriers. The genotypes of all animals were confirmed by linkage analysis using PCR-based polymorphisms closely linked to the respective mutations. When we crossed these carriers, we observed that the double homozygous mutants displayed the expanded peripheral RPE phenotype as

predicted (Fig. 5D). Therefore, the expanded RPE, reduced CMZ phenotype of *kes* is genetically epistatic to the reduced CMZ of *gog*. This suggests that *kes* may act in an earlier, more pluripotent retinal stem cell than *gog*. Alternatively, this could reflect that *kes* and *gog* act in the same cells and have similar functions, but *kes* is a more severe loss-of-function than *gog*.

Class II: Mutants with expanded CMZ

The second major class of mutants has an expanded CMZ and is subdivided into three groups. The most common group (Class II-A) is represented by nine independent lines (*she*, *rys*, and seven unnamed mutants). In these fish, the Nissl-bright region at the retinal periphery is grossly expanded (Fig. 6A). The CMZ often folds back onto itself in a U-shape (arrows in Fig. 6A). The shape of cells in the CMZ is abnormal, and the nuclei appear larger and more elongated than wild-type (Fig. 2D'). DAPI staining of the nuclei in the mutant CMZ is also often brighter than normal, suggesting that the cells could be polyploid (Fig. 6A). Five of the nine Class II-A mutants also have protrusions of the RPE central to the expanded CMZ (Table 1), but these protrusions do not completely entrap the CMZ (Fig. 2D), and it does not appear that defects in the RPE are primarily responsible for the expanded CMZ phenotype. The central embryonic retina appears normal, except for photoreceptor defects in five Class II-A mutants. In *rys*, photoreceptors have shorter outer segments centrally and are absent peripherally (Fig. 2D, 6A), whereas in *she* there are fewer photoreceptors throughout (Fig. 6I). Interestingly, the IPL and photoreceptor outer segments adjacent to the expanded marginal zone do not appear immature, but rather appear fully differentiated, suggesting

that few new cells are being added to the neural retina of this mutant despite the enlarged CMZ. When we stained *she* mutants with a marker of specific differentiated cell types, we confirmed that differentiated cells are directly apposed to the expanded CMZ (Fig. 6G). In contrast, in wild-type larvae the immature retina adjacent to the CMZ does not label with markers of differentiated cells (Fig. 6D).

One explanation for an expanded, but non-functional CMZ with elongated cells, as seen in Class II-A mutants, is that the retinal progenitors arrest in the cell cycle. To test this possibility, we examined the ability of CMZ progenitors to progress through the cell cycle using two markers, Proliferating Cell Nuclear Antigen (PCNA) and BrdU. PCNA is transiently present in the nucleus of dividing cells during G1, S, and G2 phases (Takasaki et al., 1981) and it labels most cells in the wild-type CMZ (Fig. 6E). BrdU is incorporated into DNA during S phase and the label is retained in daughter cells in a stable fashion. When we injected larvae with a pulse of BrdU at 5 dpf and sectioned at 6 dpf, robust labeling was observed in the CMZ of wild-type larvae (Fig. 6F). In the *she* mutant, the expanded Nissl-bright region labeled brightly with PCNA (Fig. 6H), but very few if any cells were labeled with BrdU (Fig. 6I). BrdU labeling was observed outside the retina in *she* larvae, such as along the brain ventricles (data not shown), again suggesting the defect is relatively specific to the retina. The reduction in BrdU labeling with maintained PCNA labeling suggests that the progenitors in *she* retina are unable to progress through S-phase and are arrested in the cell cycle.

Only one Class II-B mutant was observed (*xie*), and it also shows an expanded CMZ. The Nissl-bright region is wider than wild-type, but the cells show a normal morphology (Fig. 6B), in contrast to the mutants of Class II-A, which have elongated

nuclei. By 5 dpf, the wild-type CMZ is typically two cells wide at the level of the IPL (see Fig. 1F), whereas in *xie*, there are four or more Nissl-bright cells (Fig. 6B). The IPL and photoreceptor outer segments in *xie* mutants appear differentiated up to the central edge of the widened CMZ, suggesting that the CMZ is not productive and few new cells are differentiating. The phenotypic distinction between Class II-B and Class II-A mutants is subtle, and it is possible that the spectrum of phenotypes is really continuous. Conceivably, the *xie* phenotype could also arise from a cell cycle arrest, although perhaps at a different phase than Class II-A, because the cells in the *xie* CMZ do not display an abnormally elongated shape.

The last mutant, *bug*, is designated as Class II-C and develops a CMZ that splits into two branches (Fig. 6C). The first branch of the CMZ maintains the normal location at the peripheral margin, but the second branch curves centrally between the lens and the ganglion cell layer. The RPE also protrudes into the retina between the lens and the CMZ (asterisk in Fig. 6C). Further experimentation will be required to assess whether new cells are being added at the terminus of the ectopic CMZ. The ectopic branch suggests a shift in progenitor cell fate bias, possibly with too many ganglion cell progenitors produced.

Class I and II double mutant analysis

Based on their phenotypes, we hypothesized that the reduced CMZ Class I mutants would affect retinal stem cells and that the expanded CMZ Class II would affect retinal progenitors. We therefore predicted that a double mutant animal would exhibit the reduced CMZ phenotype, because in the absence of stem cells, progenitors cannot accumulate. We chose an exemplary mutant from the expanded CMZ Class II-A, *rys*

(Fig. 7B), and the reduced CMZ Class I-A, *gog* (Fig. 7C). We mated *rys* and *gog* to create double heterozygous carriers. The genotypes of all animals were confirmed by linkage analysis using PCR-based polymorphisms closely linked to the respective mutations. When we crossed these carriers, we observed that the double homozygous mutants displayed the reduced CMZ phenotype as predicted (Fig. 7D). Therefore, the reduced CMZ phenotype of *gog* is genetically epistatic to the expanded CMZ of *rys*. The double mutants also displayed some phenotypes characteristic of the expanded CMZ mutant, however, such as poor body posture and short photoreceptor outer segments (Fig. 7D, and data not shown). This suggests that while loss of the CMZ supersedes its expansion, the genes mutated in these two mutants are unlikely to be in a simple linear pathway.

Candidate gene linkage analysis

We mapped all eight mutants from Class I and one mutant from Class II to small chromosomal regions in order to compare their positions with the locations of genes known to regulate retinal specification, stem cells, or growth (Table 2). These included retina-enriched genes from the Rx, Six3, Pax6, Mitf, and Vsx families (Rx: Mathers et al., 1997; Six3: Loosli et al., 1999; Pax6: Hitchcock et al., 1996; Mitf: Lister et al., 2001; Vsx: Levine et al., 1997), cell cycle genes implicated in retinal progenitors such as p27Kip1, p57Kip2, and Rb (p27Kip1: Dyer and Cepko, 2001; p57Kip2: Dyer and Cepko, 2000; Rb: Zhang et al., 2004), stem cell and progenitor genes such as Delta/Notch, Jak/Stat, Wt1, Bmi1, Ncor, Nanos, and Piwi (Notch/Delta reviewed in Roth, 2001; Jak/Stat: Kiger et al., 2001, Tulina and Matunis, 2001; Wt1: Wagner et al., 2002; Bmi1:

Molofsky et al., 2003; Ncor: Hermanson et al., 2002; Nanos: Wang and Lin, 2004; Piwi: Lin and Spradling, 1997), and signaling pathways implicated in regulating growth such as IGF (reviewed in Otteson and Hitchcock, 2003). None of the mutations we found could be matched to any of the expected candidates (Table 2).

DISCUSSION

Given the enormous interest in adult stem cells, which has been boosted by their widely accepted therapeutic potential, surprisingly little is known about the gene networks that regulate their maintenance and output *in vivo*. This work reports a forward-genetic strategy to identify the genes regulating stem cells after the end of embryogenesis. We devised a two-step screening assay, first taking advantage of the functional output of these post-embryonic stem cells (growth of the retina), and second using a rigorous morphological selection for mutations specific to the retinal stem-cell compartment. The retinal stem-cell niche, the CMZ, is ideal for a high-throughput, phenotype-based genetic approach, because it is found at an invariant position in the retinal periphery. A relatively simple three-color staining paradigm reveals many facets of its architecture. Using this method, we isolated 18 mutant strains (1% of the 1,740 F2 families screened) that exhibit normal embryonic development, but fail to add new cells to the post-embryonic neural retina. An additional 46 lines (2.5%) with CMZ phenotypes were observed, but discarded for lack of specificity. We also observed at least six mutants with a subtly reduced CMZ. When we labeled these mutants with BrdU, we detected a significant reduction in cell division in the CMZ, but it was not as dramatic as in the Class I mutants described here (AMW, unpublished data). While we chose to keep only

the strongest mutants in the current screen, we believe our histological assay would be sensitive enough to detect weaker phenotypes and should be useful for further screens, including modifier screens.

It is striking that these mutations disrupt larval growth of the retina, while leaving embryonic development of the eye and other organs largely unaffected. The existence of at least 18 CMZ-specific mutants demonstrates that embryonic and post-embryonic retinal stem cells utilize separable genetic programs. There are two potential interpretations for this observation, each with different implications for the regulatory mechanisms used by stem cells. The first possibility is that post-embryonic growth of the retina is regulated by a dedicated set of genes, largely distinct from those regulating embryogenesis. These genes may act non-autonomously in the stem cell niche to recruit or maintain the undifferentiated, self-renewing population, or they may function autonomously in stem cells or progenitors. It would be exciting if our screen had uncovered genes that are used by the niche to shield stem cells from the wave of differentiation during embryogenesis or genes that influence the responsiveness of stem cells to niche-derived signals.

The second possibility is that there is substantial maternal deposition of RNAs or proteins in oocytes that are necessary for cell proliferation. The activity of these maternal products allows embryogenesis to proceed normally up to the stage when zygotic contribution becomes essential. Rapidly dividing populations of cells, particularly in greatly expanding tissues such as the retina, might deplete maternal stores more quickly than cells undergoing fewer divisions. Mutations in essential genes expressed from both the maternal and the zygotic genomes could thus give rise to tissue-specific or cell-type

specific phenotypes, such as the ones observed here. In this case, the genes controlling embryonic development could overlap greatly with those controlling larval growth. It should be noted that some of our mutants survive up to two weeks of age, while maternal stores usually do not last more than a day in zebrafish (reviewed in Pelegri, 2003). In any case, maternal effects would provide useful opportunities to study the function of essential genes in differentiated tissues and organs, a distinctive advantage of animals such as zebrafish (with large, maternally loaded eggs) over the mouse, whose embryos develop slowly and inherit fewer maternal products.

The phenotypes discovered in our screen have allowed us to place the mutated genes in a hypothetical pathway (Fig. 8). Mutations leading to a reduced CMZ (Class I) are likely to affect the post-embryonic retinal stem cells directly (or their immediate progenitor daughters). Based on the lack of proliferation and the absence of immature cells in the larval retina of these mutants, the stem cell population could be missing or mitotically quiescent. Our model (Fig. 8) predicts that Class I-A genes are either necessary for the creation of rapidly dividing progenitors, or for self-renewal of stem cells. Both defects should result in a reduced CMZ. We noted that a few cells in the CMZ still incorporated BrdU in these mutants, suggesting that some small proliferative capacity is maintained. The identity of these rare dividing cells is unknown.

Our data further suggest that Class II genes affect the retinal progenitor cells (Fig. 8). In an epistasis experiment, we found that the defect in (at least one of the) Class II-A mutants is downstream of the defect in (at least one of the) Class I-A mutants, consistent with a function of Class I genes in an early cell division event and the function of Class II genes in the later expansion and differentiation of progenitors. The extended shape and

large, elongated nuclei of CMZ cells in Class II-A mutants is characteristic of mitotic cells in telophase. Moreover, expression of the broad cell cycle marker PCNA is maintained in mutant progenitors that no longer incorporate BrdU. These observations strongly suggest that the progenitors arrest in the cell cycle and accumulate in the CMZ instead of differentiating properly. Finally, we noticed that the DAPI signal was stronger in the CMZ of Class II-A mutants, a possible sign of polyploidy. A mutation in a cell cycle regulatory gene would be predicted to result in a severe and pleiotropic phenotype (unless it is maternally provided), although there are recent reports of relatively subtle phenotypes in mice lacking all three D-type cyclins (Kozar et al., 2004). It will be interesting to investigate whether Class II-A, II-B, and II-C mutants arrest in different phases of the cell cycle, given their distinct cellular phenotypes, although most of the markers necessary for this analysis have not been applied to the zebrafish system.

In at least eight of the mutant lines isolated in our screen, the RPE also showed a phenotype, including invasion into the neural retina central to the CMZ (in Class II) or expansion in the peripheral-most RPE overlying the CMZ (in Class I-B). Thickening of the RPE is not correlated with smaller eyes, as we did not observe this phenotype in over 200 small-eyed mutants sectioned during the screen. Neural retina and RPE are thought to retain separate identities and distinct lineages throughout post-embryonic growth, after their early split into separate layers by 24 hpf. In this conventional view, the concordance of RPE and CMZ phenotypes could be due to disruption of signaling between neural retina and RPE, which normally coordinates their growth. If cell proliferation in both tissues is coordinated by shared signals then mutations that result in CMZ overgrowth may also cause overgrowth of the RPE, as seen in Class II mutants. In Class I-B mutants,

however, the RPE is enlarged and the CMZ is reduced, a phenotype that cannot be explained in a straightforward manner with a model of coordinated growth.

We therefore favor a different model, which seems to best fit all our data (Fig. 8). In this model, two neighboring proliferative populations, the CMZ and the peripheral RPE, may arise from a common stem cell in the larval eye. The existence of a stem cell capable of producing both neural retina and pigmented epithelium has been suggested previously by lineage tracing experiments in *Xenopus* tadpoles (Wetts et al., 1989). In this elegant study, single labeled cells at the CMZ/RPE boundary not only gave rise to separate clones of cells in the neural retina and the RPE, but sometimes to clones with progeny in both tissues. The hypothesis of a pan-retinal stem cell is provocative as it implies that the split of the neural retina and RPE lineages during embryogenesis is not final. Rather, the boundary zone between the two embryonic tissues, which will become the CMZ and the adjacent pigmented zone in the larval retina may continue to provide a suitable niche to maintain a sparse population of pan-retinal stem cells. These multipotent stem cells might also give rise to the ciliary and iris epithelia, two later-developing tissues, which are derivatives of the embryonic optic cup (reviewed in Chow and Lang, 2001). In this extended model, the pan-retinal stem cells reside at the interface between neural and epithelial cells throughout growth of the eye.

Another line of evidence supporting the close relationship between neural and pigmented progenitors is the capacity of the RPE to transdifferentiate into retinal neurons (reviewed in Del Rio-Tsonis and Tsonis, 2003), especially after treatment with FGF. The reverse situation, a transdifferentiation of neural retina into RPE, has also been observed recently in Chx10 null mice (Rowan et al., 2004). Furthermore, when cells were dissected

out from the retinal periphery of adult mice and cultured individually, they produced clones containing both RPE and differentiated neural cells (Tropepe et al., 2000). These *in vitro* results are consistent with our *in vivo* observations to suggest that a population of retinal stem cells exists that can generate both pigmented and neural cells.

Our genetic epistasis experiment between Class I-A and Class I-B mutants also suggests that the primary stem cell is capable of generating both pigmented and neural cells. The observation that Class I-A, Class I-B double mutants have an expanded peripheral RPE suggests that Class I-B genes function in an earlier stem cell than Class I-A genes and that the earlier stem cell can make either pigmented or neural progeny. According to this model, the phenotype of the two Class I-B mutants could be caused by a block in neuroretinal potential, such that the retinal stem cells are now restricted to the pigmented epithelial lineage. Similarly, the function of Chx10, a homeodomain transcription factor, might be to bias the retinal stem cell to the neural lineage (Rowan et al., 2004). The basic helix-loop-helix factor Mitf may serve the reciprocal role of committing the retinal stem-cell progeny to the pigmented epithelial fate (Lister et al., 2001). While loss-of-function of Chx10 (Vsx2) and gain-of-function in one of the two zebrafish Mitf genes are good candidates for a Class I-B mutation, the map positions of these genes do not correspond with any of the mutations discovered here.

Several genetic and biochemical pathways have been implicated in regulating stem cells, but none have been demonstrated to act in adult somatic stem cells *in vivo*. Perhaps surprisingly, we found that the mutated genes isolated in our screen are not components of previously studied pathways. Although our panel of mutations is certainly not exhaustive, given that our screen was not saturating, it is still provocative that none of

them disrupts expected candidate genes. The cloning and characterization of the underlying genes should therefore provide novel insights into the mechanisms by which stem cells, both in the eye and in other organs of the body, are maintained after embryogenesis.

EXPERIMENTAL PROCEDURES

Genetic techniques

Fish were maintained at 28°C. Chemical mutagenesis with N-ethyl-N-nitrosourea (ENU) was performed as in van Eeden et al., (1999). All mutants are recessive and were generated by intercrossing heterozygous carriers. Fish were maintained in the TL genetic background except for linkage mapping experiments, in which they were crossed to the WIK strain. Mapping was performed as in Kay et al., (2001) using the MGH microsatellite map (Shimoda et al., (1999), the consolidated mapping data provided by the Zebrafish Information Network (Sprague et al., (2001); www.zfin.org), and the zebrafish genome project (www.sanger.ac.uk/ Projects/D_rerio/ and www.ensembl.org/Danio_rerio/).

Fluorescent Nissl/DAPI staining

Larvae were fixed in 4% paraformaldehyde (PFA) in phosphate-buffered saline (PBS), then cryoprotected in 30% Sucrose/0.02%Sodium Azide before sectioning at 12μm horizontally or transversely on a cryostat. Slides were rehydrated in PBS, incubated in 1:50 NeuroTrace™ Nissl (Molecular Probes) in PBS for 30 min, washed

two times with PBS, stained in 1:100 4'-6-diamino-2-phenylindole (DAPI) in water for 1 min, coverslipped using fluorescent mounting media and dried overnight before photographing with a cooled-CCD camera (SPOT-RT, Diagnostic Instruments). Immunohistochemistry was performed as in Kay et al., (2001). We used rat anti-BrdU (1:200; Accurate Chemicals); anti-PCNA (Sigma-Aldrich, 1:1000); and anti-calretinin (Chemicon, 1:1000). For PCNA labeling, retinas were fixed in 4% PFA in ethanol.

Plastic sections

Larvae were fixed at 6 dpf in 1% paraformaldehyde - 2.5% glutaraldehyde in phosphate buffer overnight at 4°C. Larvae were then dehydrated through a methanol series into acetone, embedded in Eponate 12 resin (Ted Pella, Redding, CA), and cured for 2 days at 65°C. Horizontal sections (1 μm) were collected using an ultramicrotome (Reichert-Jung) and stained with 1% azure II - 1% methylene blue in 1% sodium borate and coverslipped with Permount (Fisher).

BrdU labeling

To examine cell proliferation, larvae were incubated in the thymidine analog 5-bromo-2-deoxyuridine (BrdU) at 2mM in embryo medium for 12 hours then returned to embryo medium without BrdU for at least one day (figures 3 and 4). For the experiment in figure 5, larvae were injected with 10mM BrdU in PBS (with 0.1% Phenol Red) at 5 dpf and fixed in 4% PFA 1 day later. Approximately 5 nl BrdU was injected into the residual yolk sac.

ACKNOWLEDGEMENTS

The authors would like to acknowledge Kerry Deere, D. Ana Mrejeru, Anna Reichardt, and Victoria Kahn for technical assistance. We also thank members of the Baier and Stainier labs for their participation in the screen effort. We would also like to thank Ellie Heckscher and members of the Baier lab for their comments on the manuscript. AMW was funded by an ARCS fellowship and an AAUW Educational Foundation American Dissertation fellowship. JRM was funded by a Ruth Kirschstein NRSA fellowship, with support from NIH EY04318 (PAR). This work was funded by NIH EY13855 and a David and Lucile Packard Fellowship (HB).

REFERENCES

Ahmad, I., Tang, L., and Pham, H. (2000). Identification of neural progenitors in the adult mammalian eye. *Biochem Biophys Res Commun* **270,** 517-21.

Chow, R. L., and Lang, R. A. (2001). Early eye development in vertebrates. *Annu Rev Cell Dev Biol* **17,** 255-96.

Cogle, C. R., Guthrie, S. M., Sanders, R. C., Allen, W. L., Scott, E. W., and Petersen, B. E. (2003). An overview of stem cell research and regulatory issues. *Mayo Clin Proc* **78,** 993-1003.

Del Rio-Tsonis, K., and Tsonis, P. A. (2003). Eye regeneration at the molecular age. *Dev Dyn* **226,** 211-24.

Dyer, M. A., and Cepko, C. L. (2000). Control of Muller glial cell proliferation and activation following retinal injury. *Nat Neurosci* **3,** 873-80.

Dyer, M. A., and Cepko, C. L. (2001). p27Kip1 and p57Kip2 regulate proliferation in distinct retinal progenitor cell populations. *J Neurosci* **21,** 4259-71.

Easter, S. S., Jr., and Malicki, J. J. (2002). The zebrafish eye: developmental and genetic analysis. *Results Probl Cell Differ* **40,** 346-70.

Fadool, J. M., Brockerhoff, S. E., Hyatt, G. A., and Dowling, J. E. (1997). Mutations affecting eye morphology in the developing zebrafish (Danio rerio). *Dev Genet* **20,** 288-95.

Fuchs, E., Tumbar, T., and Guasch, G. (2004). Socializing with the neighbors: stem cells and their niche. *Cell* **116,** 769-78.

Golling, G., Amsterdam, A., Sun, Z., Antonelli, M., Maldonado, E., Chen, W., Burgess, S., Haldi, M., Artzt, K., Farrington, S., Lin, S. Y., Nissen, R. M., and Hopkins, N. (2002). Insertional mutagenesis in zebrafish rapidly identifies genes essential for early vertebrate development. *Nat Genet* **31,** 135-40.

Haffter, P., Granato, M., Brand, M., Mullins, M. C., Hammerschmidt, M., Kane, D. A., Odenthal, J., van Eeden, F. J., Jiang, Y. J., Heisenberg, C. P., Kelsh, R. N., Furutani-Seiki, M., Vogelsang, E., Beuchle, D., Schach, U., Fabian, C., and Nusslein-Volhard, C. (1996). The identification of genes with unique and essential functions in the development of the zebrafish, Danio rerio. *Development* **123,** 1-36.

Harris, W. A., and Perron, M. (1998). Molecular recapitulation: the growth of the vertebrate retina. *Int J Dev Biol* **42,** 299-304.

Hermanson, O., Jepsen, K., and Rosenfeld, M. G. (2002). N-CoR controls differentiation of neural stem cells into astrocytes. *Nature* **419,** 934-9.

Hitchcock, P., Ochocinska, M., Sieh, A., and Otteson, D. (2004). Persistent and injury-induced neurogenesis in the vertebrate retina. *Prog Retin Eye Res* **23,** 183-94.

Hitchcock, P. F., Macdonald, R. E., VanDeRyt, J. T., and Wilson, S. W. (1996). Antibodies against Pax6 immunostain amacrine and ganglion cells and neuronal progenitors, but not rod precursors, in the normal and regenerating retina of the goldfish. *J Neurobiol* **29,** 399-413.

Ivanova, N. B., Dimos, J. T., Schaniel, C., Hackney, J. A., Moore, K. A., and Lemischka, I. R. (2002). A stem cell molecular signature. *Science* **298,** 601-4.

Kay, J. N., Finger-Baier, K. C., Roeser, T., Staub, W., and Baier, H. (2001). Retinal ganglion cell genesis requires lakritz, a Zebrafish atonal Homolog. *Neuron* **30,** 725-36.

Kiger, A. A., Jones, D. L., Schulz, C., Rogers, M. B., and Fuller, M. T. (2001). Stem cell self-renewal specified by JAK-STAT activation in response to a support cell cue. *Science* **294,** 2542-5.

Kozar, K., Ciemerych, M. A., Rebel, V. I., Shigematsu, H., Zagozdzon, A., Sicinska, E., Geng, Y., Yu, Q., Bhattacharya, S., Bronson, R. T., Akashi, K., and Sicinski, P. (2004). Mouse development and cell proliferation in the absence of D-cyclins. *Cell* **118,** 477-91.

Kubota, R., Hokoc, J. N., Moshiri, A., McGuire, C., and Reh, T. A. (2002). A comparative study of neurogenesis in the retinal ciliary marginal zone of homeothermic vertebrates. *Brain Res Dev Brain Res* **134,** 31-41.

Levine, E. M., Passini, M., Hitchcock, P. F., Glasgow, E., and Schechter, N. (1997). Vsx-1 and Vsx-2: two Chx10-like homeobox genes expressed in overlapping domains in the adult goldfish retina. *J Comp Neurol* **387,** 439-48.

Li, Z., Joseph, N. M., and Easter, S. S., Jr. (2000). The morphogenesis of the zebrafish eye, including a fate map of the optic vesicle. *Dev Dyn* **218,** 175-88.

Lin, H., and Spradling, A. C. (1997). A novel group of pumilio mutations affects the asymmetric division of germline stem cells in the Drosophila ovary. *Development* **124,** 2463-76.

Lister, J. A., Close, J., and Raible, D. W. (2001). Duplicate mitf genes in zebrafish: complementary expression and conservation of melanogenic potential. *Dev Biol* **237,** 333-44.

Loosli, F., Winkler, S., and Wittbrodt, J. (1999). Six3 overexpression initiates the formation of ectopic retina. *Genes Dev* **13,** 649-54.

Malicki, J., Neuhauss, S. C., Schier, A. F., Solnica-Krezel, L., Stemple, D. L., Stainier, D. Y., Abdelilah, S., Zwartkruis, F., Rangini, Z., and Driever, W. (1996). Mutations affecting development of the zebrafish retina. *Development* **123,** 263-73.

Marcus, R. C., Delaney, C. L., and Easter, S. S., Jr. (1999). Neurogenesis in the visual system of embryonic and adult zebrafish (Danio rerio). off. *Vis Neurosci* **16,** 417-24.

Mathers, P. H., Grinberg, A., Mahon, K. A., and Jamrich, M. (1997). The Rx homeobox gene is essential for vertebrate eye development. *Nature* **387,** 603-7.

Molofsky, A. V., Pardal, R., Iwashita, T., Park, I. K., Clarke, M. F., and Morrison, S. J. (2003). Bmi-1 dependence distinguishes neural stem cell self-renewal from progenitor proliferation. *Nature* **425,** 962-7.

Neuhauss, S. C., Biehlmaier, O., Seeliger, M. W., Das, T., Kohler, K., Harris, W. A., and Baier, H. (1999). Genetic disorders of vision revealed by a behavioral screen of 400 essential loci in zebrafish. *J Neurosci* **19,** 8603-15.

Otteson, D. C., and Hitchcock, P. F. (2003). Stem cells in the teleost retina: persistent neurogenesis and injury-induced regeneration. *Vision Res* **43,** 927-36.

Page-McCaw, P. S., Chung, S. C., Muto, A., Roeser, T., Staub, W., Finger-Baier, K. C., Korenbrot, J. I., and Baier, H. (2004). Retinal network adaptation to bright light requires tyrosinase. *Nat Neurosci* **7,** 1329-36.

Patton, E. E., and Zon, L. I. (2001). The art and design of genetic screens: zebrafish. *Nat Rev Genet* **2,** 956-66.

Pelegri, F. (2003). Maternal factors in zebrafish development. *Dev Dyn* **228,** 535-54.

Perron, M., Kanekar, S., Vetter, M. L., and Harris, W. A. (1998). The genetic sequence of retinal development in the ciliary margin of the Xenopus eye. *Dev Biol* **199,** 185-200.

Ramalho-Santos, M., Yoon, S., Matsuzaki, Y., Mulligan, R. C., and Melton, D. A. (2002). "Stemness": transcriptional profiling of embryonic and adult stem cells. *Science* **298,** 597-600.

Roth, S. (2001). Drosophila oogenesis: coordinating germ line and soma. *Curr Biol* **11,** R779-81.

Rowan, S., Chen, C. M., Young, T. L., Fisher, D. E., and Cepko, C. L. (2004). Transdifferentiation of the retina into pigmented cells in ocular retardation mice defines a new function of the homeodomain gene Chx10. *Development* **131,** 5139-52.

Schmitt, E. A., and Dowling, J. E. (1994). Early eye morphogenesis in the zebrafish, Brachydanio rerio. *J Comp Neurol* **344,** 532-42.

Shimoda, N., Knapik, E. W., Ziniti, J., Sim, C., Yamada, E., Kaplan, S., Jackson, D., de Sauvage, F., Jacob, H., and Fishman, M. C. (1999). Zebrafish genetic map with 2000 microsatellite markers. *Genomics* **58,** 219-32.

Sprague, J., Doerry, E., Douglas, S., and Westerfield, M. (2001). The Zebrafish Information Network (ZFIN): a resource for genetic, genomic and developmental research. *Nucleic Acids Res* **29,** 87-90.

Stappenbeck, T. S., Mills, J. C., and Gordon, J. I. (2003). Molecular features of adult mouse small intestinal epithelial progenitors. *Proc Natl Acad Sci U S A* **100,** 1004-9.

Takasaki, Y., Deng, J. S., and Tan, E. M. (1981). A nuclear antigen associated with cell proliferation and blast transformation. *J Exp Med* **154,** 1899-909.

Tropepe, V., Coles, B. L., Chiasson, B. J., Horsford, D. J., Elia, A. J., McInnes, R. R., and van der Kooy, D. (2000). Retinal stem cells in the adult mammalian eye. *Science* **287,** 2032-6.

Tulina, N., and Matunis, E. (2001). Control of stem cell self-renewal in Drosophila spermatogenesis by JAK-STAT signaling. *Science* **294,** 2546-9.

Tumbar, T., Guasch, G., Greco, V., Blanpain, C., Lowry, W. E., Rendl, M., and Fuchs, E. (2004). Defining the epithelial stem cell niche in skin. *Science* **303,** 359-63.

van Eeden, F. J., Granato, M., Odenthal, J., and Haffter, P. (1999). Developmental mutant screens in the zebrafish. *Methods Cell Biol* **60,** 21-41.

Vihtelic, T. S., and Hyde, D. R. (2002). Zebrafish mutagenesis yields eye morphological mutants with retinal and lens defects. *Vision Res* **42,** 535-40.

Wagner, K. D., Wagner, N., Vidal, V. P., Schley, G., Wilhelm, D., Schedl, A., Englert, C., and Scholz, H. (2002). The Wilms' tumor gene Wt1 is required for normal development of the retina. *Embo J* **21,** 1398-405.

Wang, Z., and Lin, H. (2004). Nanos maintains germline stem cell self-renewal by preventing differentiation. *Science* **303,** 2016-9.

Wetts, R., Serbedzija, G. N., and Fraser, S. E. (1989). Cell lineage analysis reveals multipotent precursors in the ciliary margin of the frog retina. *Dev Biol* **136,** 254-63.

Zhang, J., Gray, J., Wu, L., Leone, G., Rowan, S., Cepko, C. L., Zhu, X., Craft, C. M., and Dyer, M. A. (2004). Rb regulates proliferation and rod photoreceptor development in the mouse retina. *Nat Genet* **36,** 351-60.

Table 1

Mutations affecting post-embryonic growth of the retina

Gene	Allele	Other phenotypes
Class I-A–reduced CMZ		
gog	*s109*	
woo	*s110*	
zea	*s156*	Edema
vij	*s514, s517*	
yol	*s1504*	Lens degeneration
Class I-B–reduced CMZ, expanded peripheral RPE		
oui	*s312*	
kes	*s546*	
Class II-A–expanded CMZ–folded		
rys	*s108*	Short PhR outer segments, RPE invades central to CMZ
s111	*s111*	RPE invades central to CMZ
s168	*s168*	Short PhR outer segments, RPE invades central to CMZ
s181	*s181*	
s332	*s332*	Few PhRs with short outer segments, RPE invades central to CMZ
s507	*s507*	Few PhRs with short outer segments
s509	*s509*	
she	*s545*	Few PhRs with short outer segments, RPE invades central to CMZ
s547	*s547*	
Class II-B–expanded CMZ–dispersed		
xie	*s328*	
Class II-C–expanded CMZ–split		
bug	*s309*	PhRs rarely observed, RPE invades next to lens and central to CMZ

Note. Eleven mutants are named after films with short titles, the remaining seven are unnamed.
CMZ—ciliary marginal zone.
PhR—photoreceptors.
RPE—retinal pigmented epithelium.

Table 2

Comparison of mutants and stem-cell regulatory genes

Chromosome	Gene	Position (cM)
1	DeltaA	66-67
2	Bmi1b	43
2	Rx2	86
3	Notch3	69
3	Stat3	41-42
3	Stat5.1	41-42
4	IGF1	59-60
5	DeltaB	53
5	*gog*	61
5	Notch1B	77
5	Insulin	53 54
5	Jak2b	64-76
5	Her1	80
5	Her7	80
6	IGFBP2	45-47
6	Jak1	49
6	Her6	54
6	Mitfa	54-60
7	Pax6b	30
7	IGF1Rb	30-34
7	Her8b	39-40
7	IGF2	53
7	p57Kip2	53
8	Notch2	50-52
8	Ncor2	54-65
8	Her3	62-65
8	Piwi	66
9	*rys*	35-40
9	*vij*	55
9	Stat1b	60-64
11	Her2	63
12	Stat5.2	41
12	Six3b	42-43
13	DeltaD	30
13	Six3a	40
13	*oui*	43-70 (inversion)
13	*woo*	56-70
13	Mitfb	80
14	Her5	53
15	DeltaC	50-51
16	*kes*	27-34
17	Vsx1	41
17	Vsx2	43
18	IGF1Ra	39-41
19	Nanos	1
19	Her8a	49-51
20	*zea*	64-66
21	Jak2a	2-4
21	Notch1A	18
21	Rb1	37-38
21	Rx3	45
22	Rx1	12-15
22	Stat1	20-24
23	Her4	32
23	Her9	32
23	*yol*	42
23	Notch	45
24	Bmi1a	43
25	p27Kip1	6
25	Wt1	30-36
25	Pax6a	36
25	IGF2	39

Positions are based on the MGH microsatellite map current as of publishing.

FIGURE LEGENDS

Figure 1. Methods used in the screen to assess eye size and retinal morphology. (A) Dorsal view of a wild-type larva at 7 dpf. (B) Dorsal view of a small-eyed mutant, *yol*^{s1504}, at 7 dpf. Arrows in (A-B) point to eyes. Note that the *yol*^{s1504} larva appears grossly normal and the swim bladder is inflated (asterisk). (C-F) Triple staining of horizontal sections of 5 dpf wild-type PTU-treated eye. The CMZ resides between the paired arrows. (C) Fluorescent Nissl dye stains the CMZ most brightly (arrows mark the ends of the CMZ), but also labels ganglion and amacrine cells. (D) Autofluorescence labels the synaptic layers (i.e. the IPL) and the outer segments of the photoreceptors (POS) in paraformaldehyde-fixed sections. (E) The morphology of the CMZ (between arrows) is also apparent in DAPI-stained nuclei. (F) The merged view allows lamination of the retina to be assessed easily. All sections are oriented nasal up, temporal down. L: Lens. Scale bar in A-B, 250 μm. Scale bar in C-F, 50 μm.

Figure 2. Semi-thin plastic sections demonstrate the cellular morphology of the CMZ in mutants. (A-D) Methylene-blue stained horizontal sections of the 6 dpf larval retina. (A'-D') Magnifications of the boxed areas from (A-D). The CMZ is between the paired arrowheads. (A & A') Wild-type. (B & B') Class I-A mutant, *gog*^{s109}. Note the reduced number of undifferentiated cells at the retinal periphery. (C & C') Class I-B mutant, *kes*^{s546}. Note the expansion of the peripheral RPE (asterisks) and the reduced number of undifferentiated cells at the retinal periphery marked by the arrowheads. (D & D') Class II-A mutant, *rys*^{s108}. Note the abnormally elongated morphology of cells accumulating in

the CMZ and the invading RPE marked by an asterisk. ON: Optic nerve. Scale bar in (A-D), 50 μm. Scale bar in (A'-D'), 10 μm.

Figure 3. Class I-A mutants lack a CMZ and have a reduced number of undifferentiated and dividing cells. (A) Triple-stained wild-type eye at 6 dpf. The paired arrows mark the extent of the CMZ and the bar measures the distance between the RPE and the IPL. (B) Triple-stained *vij*^{s517} mutant at 6 dpf. Note the absence of bright Nissl staining at the peripheral edge of the retina and the reduced distance between the RPE and IPL (bar). (C) Wild-type eye double-stained for PKC-ß (green) and zpr1 (red) at 6 dpf. The bar measures the distance between the RPE and cells expressing markers of differentiated retinal neurons. (D) *yot*^{s1504} mutant eye stained for PKC-ß (green) and zpr1 (red) at 6 dpf. Note the reduced distance between the RPE and differentiated retinal neurons (bar). (E) A wild-type eye stained for BrdU incorporation at 5 dpf. Larvae were bath-treated with BrdU for 12 hours on 3 dpf. The bar marks the width of labeled cells. (F) A *vij*^{s517} mutant eye stained for BrdU incorporation at 5 dpf. The number of dividing cells is greatly reduced in *vij* (bar). Scale bar, 50 μm.

Figure 4. Class I-B mutants lack a CMZ, and the RPE is larger at the peripheral edge of the retina. (A) Triple-stained wild-type eye at 7 dpf. The CMZ is marked with paired arrows and the bar measures the distance between the RPE and the IPL. (B) Triple-stained *oui*^{s312} mutant at 7 dpf shows no Nissl-bright CMZ. The expanded RPE is labeled with an asterisk and the distance between the RPE and IPL is reduced (bar). (C) Brightfield image of wild-type eye at 5 dpf. (D) Brightfield image of *kes*^{s546} mutant at 5 dpf. The expanded RPE is labeled with an asterisk. (E) Wild-type eye stained for BrdU

incorporation at 5 dpf. Larvae were bath-treated with BrdU for 12 hours on 3 dpf. The bar measures the extent of proliferating cells. (F) A *kes*^{s546} mutant eye stained for BrdU at 5 dpf. Few cell divide in the retina of *kes*^{s546} (bar), and the expanded RPE is labeled with an asterisk. L: Lens. Scale bar, 50 μm.

Figure 5. The reduced CMZ, expanded RPE phenotype is genetically epistatic to the reduced CMZ phenotype. (A) Triple-stained wild-type eye at 4 dpf. The CMZ is marked with a paired set of arrows. (B) A triple-stained *gog*^{s109} mutant at 4 dpf shows a reduced CMZ (between arrows) and a normal RPE. (C) A triple-stained mutant *kes*^{s546} at 4 dpf shows a reduced CMZ (between arrows) and expanded peripheral RPE (asterisk). (D) Triple-stained double homozygous *gog*^{s109}/*kes*^{s546} mutant at 4 dpf. Double mutant shows the reduced CMZ phenotype of *gog*^{s109} and *kes*^{s546} (between arrows), but the expanded peripheral RPE phenotype of *kes*^{s546} (asterisk). Scale bar, 50 μm.

Figure 6. Class II mutants have an expanded CMZ. (A) Triple-stained *rys*^{s108} mutant at 5 dpf. The CMZ is expanded and folds on itself in a U-shape (between the arrows). The RPE protrudes into the neural retina at the central edge of the CMZ (asterisk). (B) A triple-stained *xie*^{s328} mutant at 5 dpf shows an expanded, wider CMZ (between arrows). (C) A triple-stained *bug*^{s309} mutant at 5 dpf has a split CMZ. One branch maintains the normal peripheral position of the CMZ (between the arrows). The second branch lies between the lens and the ganglion cell layer (arrowhead). The RPE protrudes into the retina between the CMZ and the lens (asterisk). (D) Calretinin staining in a wild-type 6 dpf retina. (E) Same section as D stained for PCNA. The arrows mark the CMZ. (F)

BrdU labeling of a wild-type retina injected with BrdU at 5 dpf and fixed at 6 dpf. (G) Calretinin staining in a *she*^{s545} retina at 6 dpf demonstrates normal differentiation of the central retina. (H) PCNA staining of the same section as G labels the enlarged U-shaped CMZ (arrows). (I) BrdU labeling of a *she*^{s545} retina injected with BrdU at 5 dpf and fixed at 6 dpf. Few cells in the CMZ are labeled indicating that they do not cycle through S-phase, although they are PCNA-positive. Asterisks mark RPE protrusion into the retina. Sections in (D-I) are transverse, with dorsal up. Scale bar, 50 μm.

Figure 7. The reduced CMZ phenotype is genetically epistatic to the expanded CMZ phenotype. (A) Triple-stained wild-type eye at 5 dpf. The CMZ is marked with a paired set of arrows and the length of the outer segments of the photoreceptors is marked with a bar. (B) A triple-stained *rys*^{s108} mutant at 5 dpf shows an expanded CMZ (between the arrows), the RPE protruding into the neural retina (asterisk), and short photoreceptors (bar). (C) A triple-stained mutant *gog*^{s109} at 5 dpf shows a reduced CMZ (between the arrows) and normal photoreceptors (bar). (D) Triple-stained double homozygous *rys*^{s108}/*gog*^{s109} mutant at 5 dpf. Double mutant shows the reduced CMZ phenotype of *gog*^{s109} (between the arrows), but the short photoreceptor phenotype of *rys*^{s108} (bar). Scale bar, 50 μm.

Figure 8. Model of post-embryonic retinal growth. A pan-retinal stem cell (RSC) divides to self-renew, to form a pigmented progenitor (PP), or to produce a neuroretinal stem cell (NSC). The pigmented progenitor divides to form several retinal pigmented epithelium (RPE) cells. The neuroretinal stem cell divides to self-renew and to give rise to an

amplifying neuroretinal progenitor population (NP). These progenitors in turn divide and differentiate to give rise to the seven cell types of the neural retina (only retinal ganglion cells (RGC), Müller glia (G), and photoreceptors (PhR) are shown). We expect the Class I-B genes to act in the retinal stem cell, Class I-A genes to act in the neuroretinal stem cell, and Class II genes to act in neuroretinal progenitor cells.

Figure 1

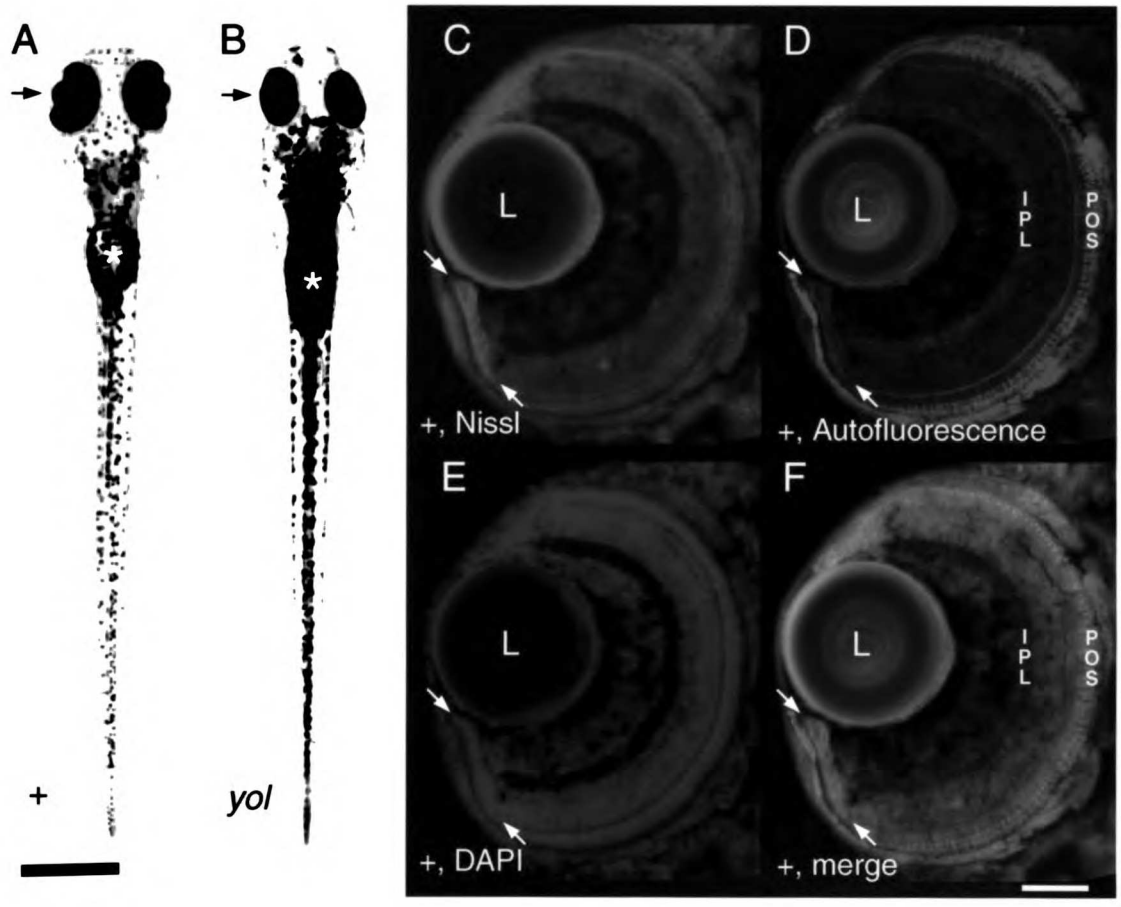

Figure 2

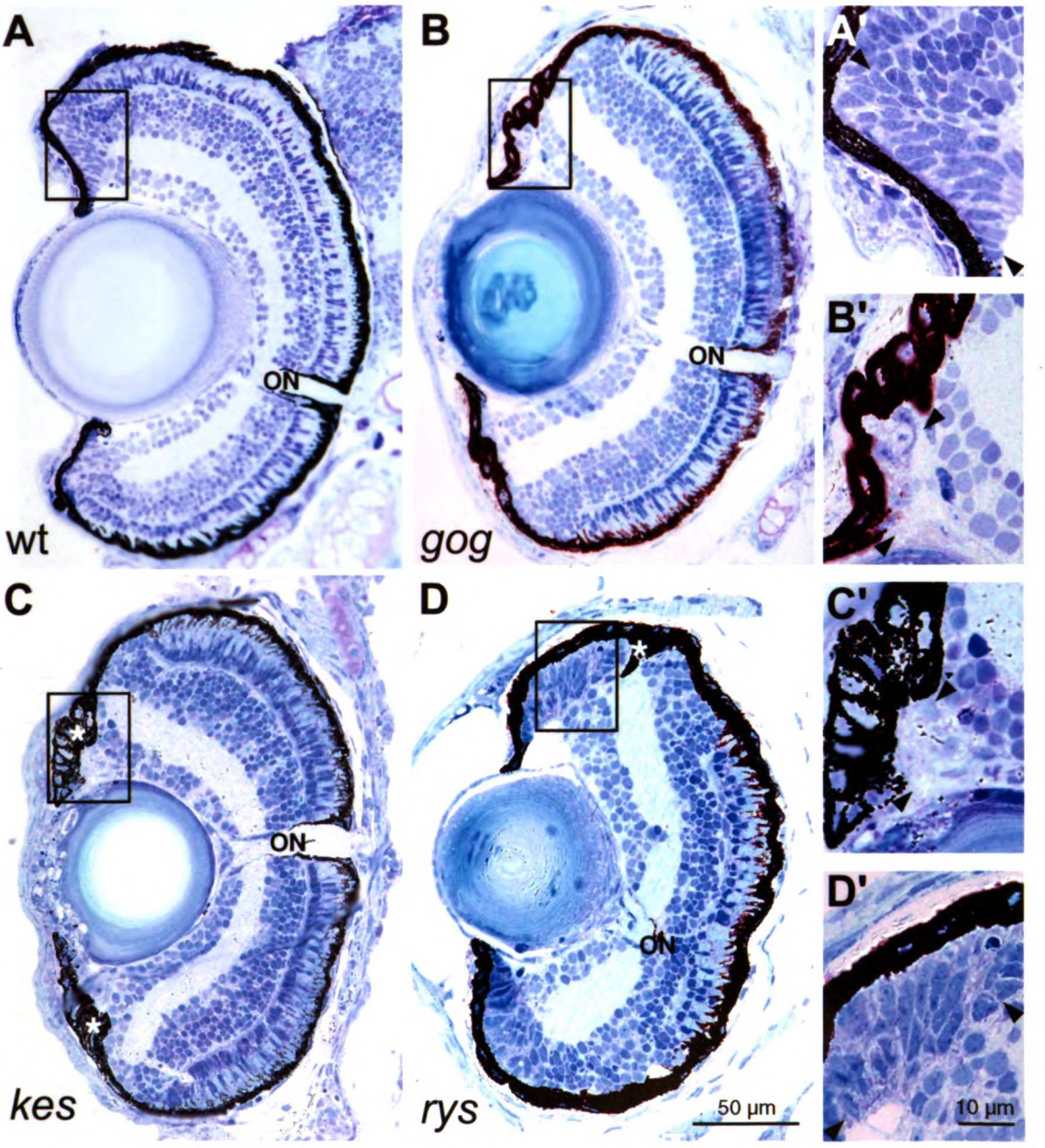

Figure 3

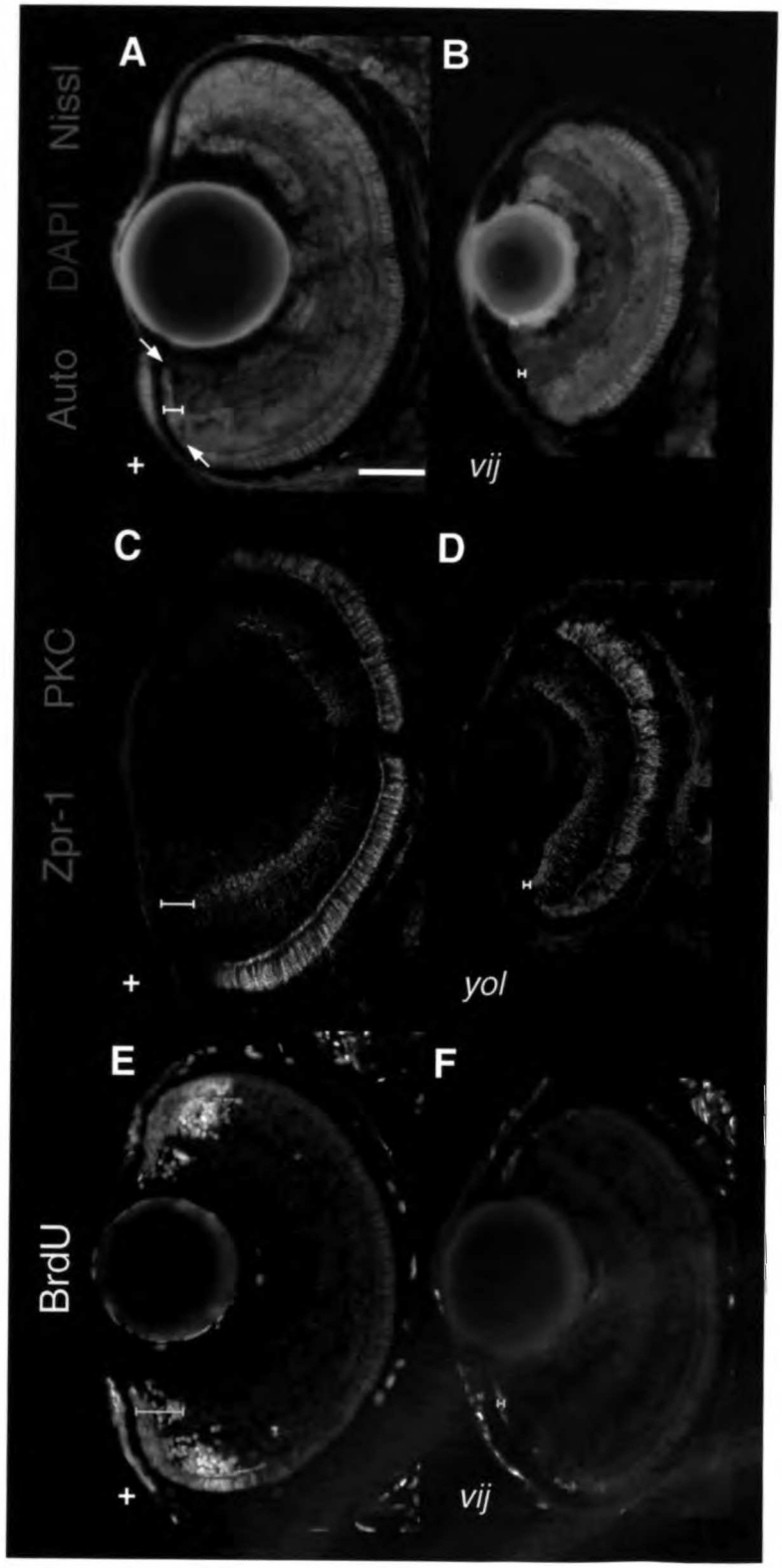

Figure 4

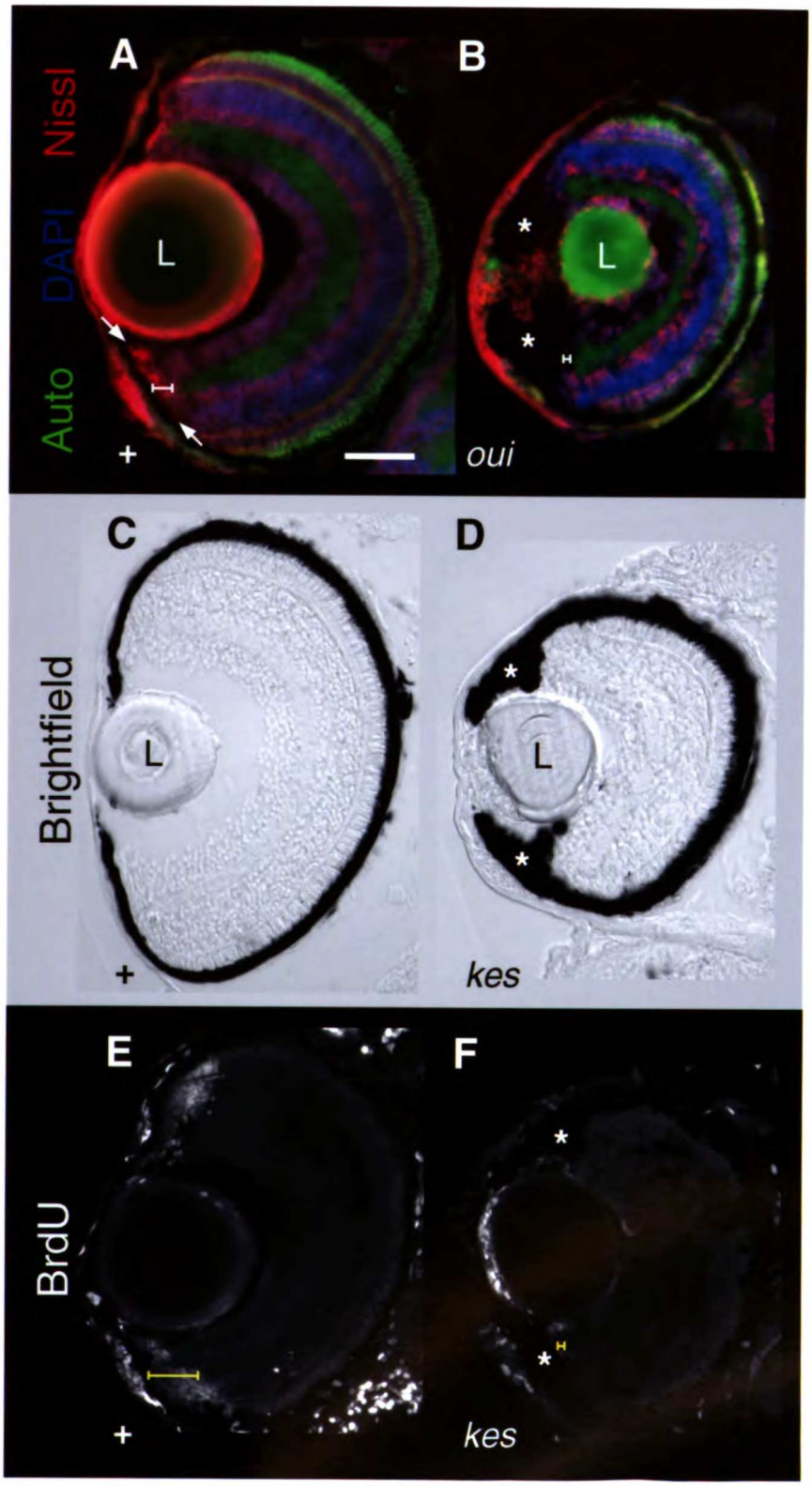

Figure 5

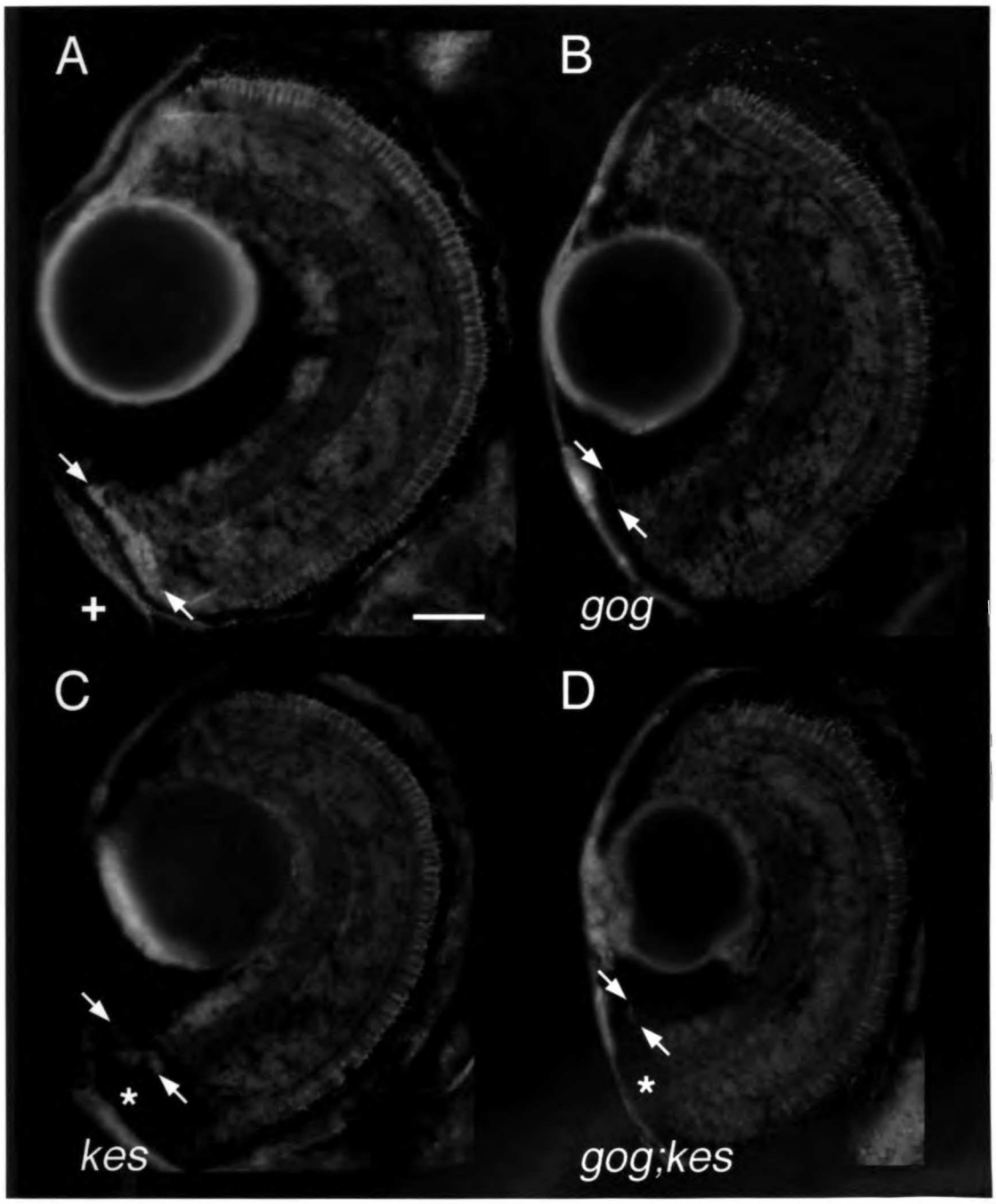

Figure 6

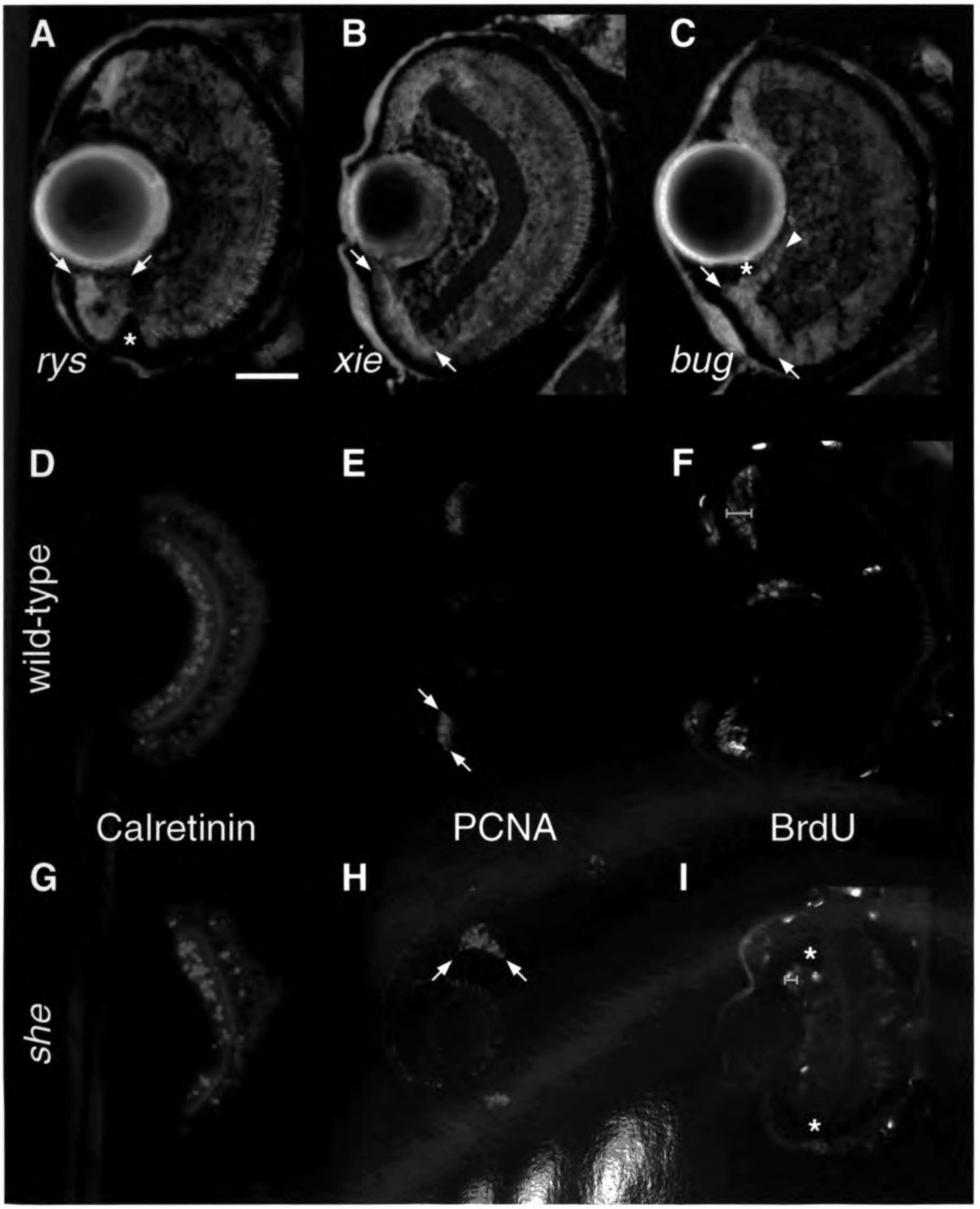

Figure 7

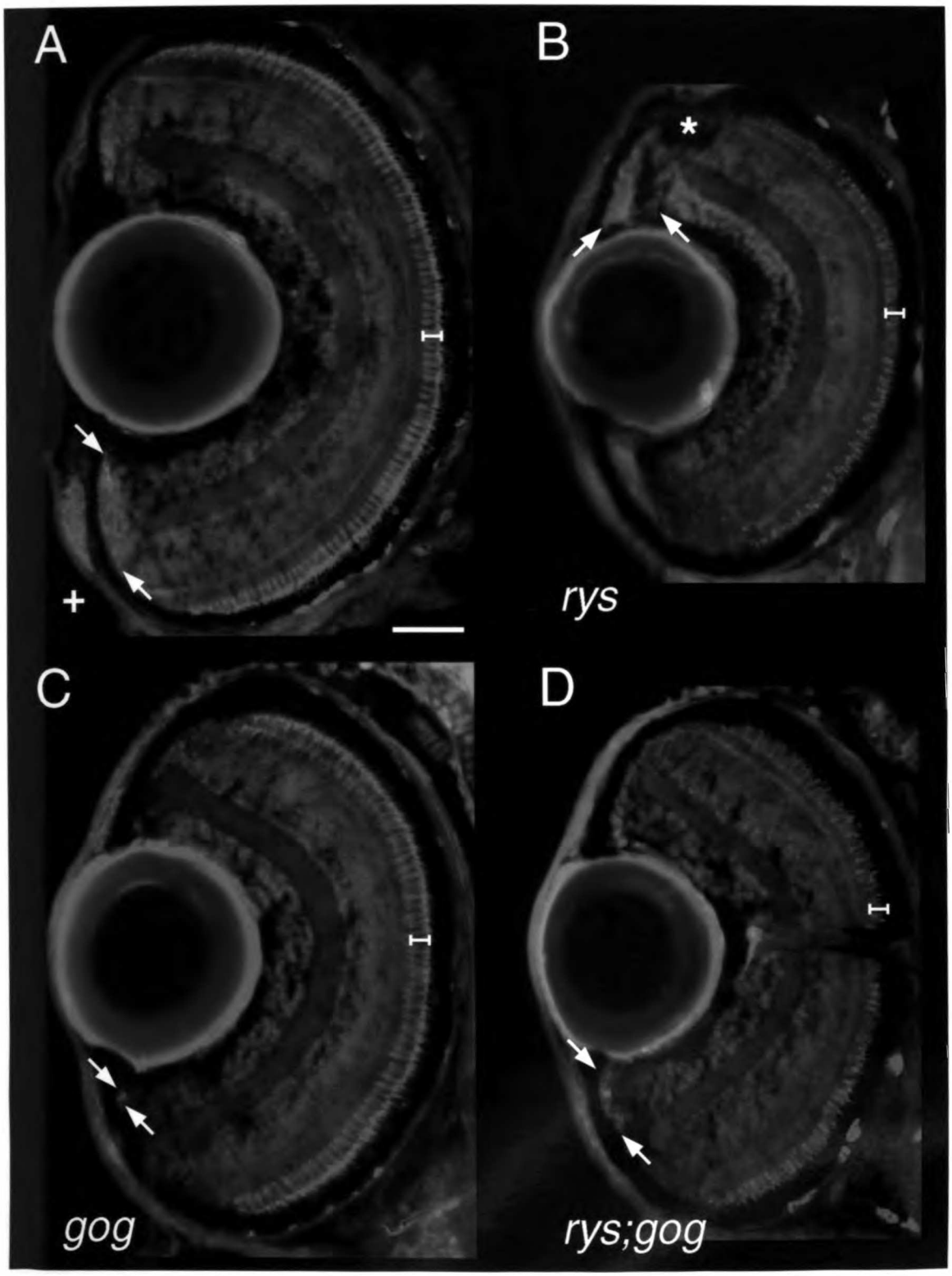

Figure 8

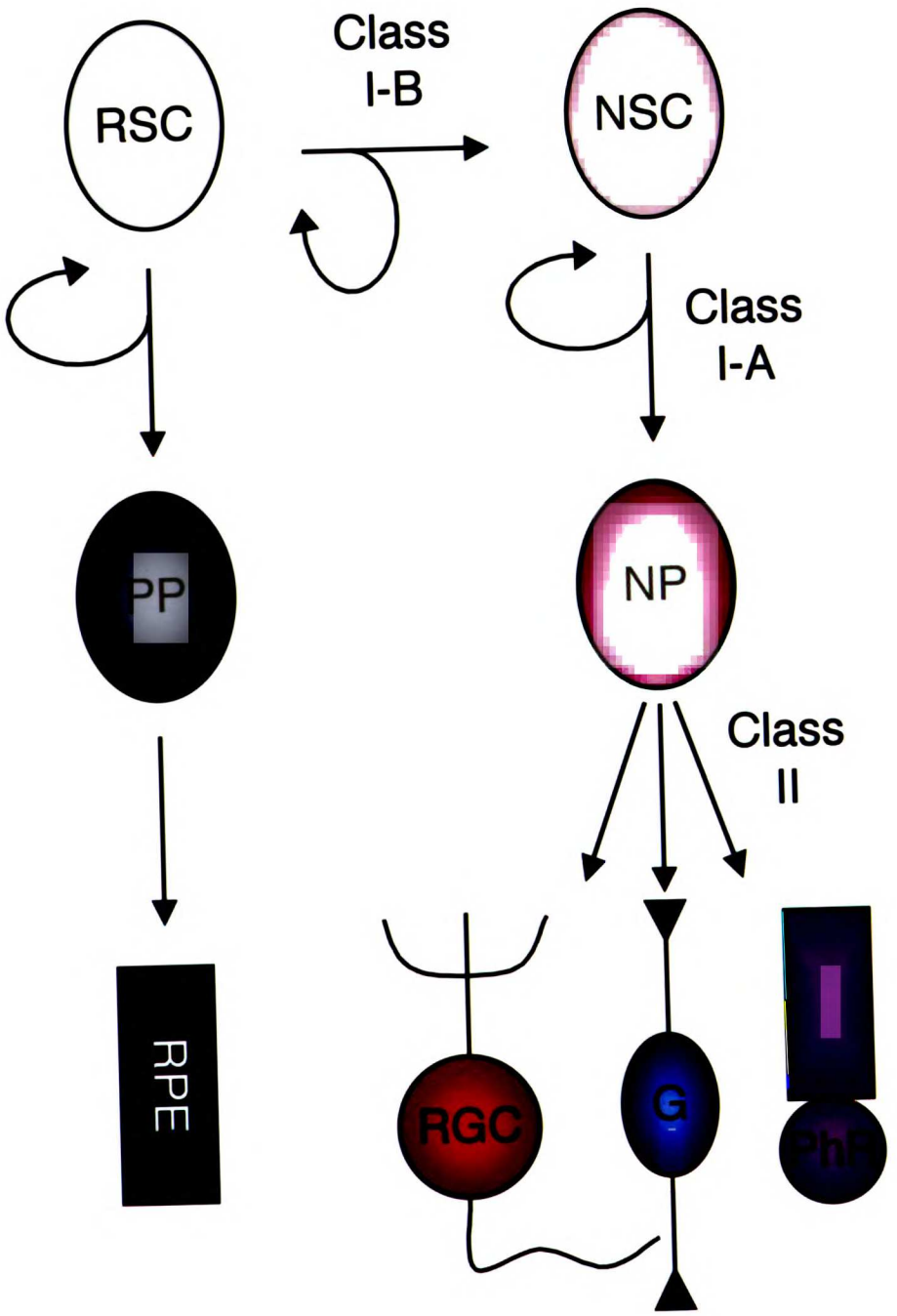

CHAPTER 2

The anaphase-promoting complex is required in both dividing and quiescent cells during zebrafish development

SUMMARY

The anaphase-promoting complex / cyclosome (APC/C) regulates multiple stages of the cell cycle, most prominently mitosis. We describe zebrafish with mutations in two APC/C subunits, Cdc16 and Cdc26, whose phenotypes reveal several characteristics of the APC/C in vertebrates. First, loss of the APC/C in dividing cells results in mitotic arrest and apoptosis. Second, subunits of the APC/C are stable proteins with maternally-deposited RNA or protein resulting in functional APC/C protein over a week later. Third, loss of the APC/C in quiescent or differentiated cells results in improper re-entry into the cell cycle. This study is the first demonstration of all three characteristics in a vertebrate organism and also provides insight into the surprisingly complex developmental phenotypes that can arise from mutation of essential genes that are maternally supplied.

CHAPTER 2

INTRODUCTION

The anaphase-promoting complex or cyclosome (APC/C) is an essential regulator of multiple steps of the cell cycle (reviewed in Zachariae and Nasmyth, 1999; Morgan, 1999). The APC/C is an E3 ubiquitin ligase that targets proteins for degradation by the 26S proteasome. Some of the best-studied targets of the APC/C are the B-type mitotic cyclins (Glotzer et al., 1991; Hershko et al., 1991). Cyclin B levels are regulated throughout the cell cycle (Evans et al., 1983). Low levels of cyclin B are maintained during G_1 and cyclin B accumulation coincides with DNA synthesis. Degradation of cyclin B is important for the progression of mitosis and its clearance is complete by the end of anaphase (Murray and Kirschner, 1989; Murray et al., 1989). This dynamic regulation of cyclin B protein levels is accomplished by APC/C-mediated proteolysis. The APC/C has multiple targets besides cyclins, most of which also regulate the cell cycle and need to be degraded in order for a cell to progress through anaphase, exit mitosis, and/or maintain G_1 (reviewed in Castro et al., 2005).

The APC/C has at least thirteen subunits and two activators (reviewed in Harper et al., 2002). APC2 is the core catalytic subunit with a cullin homology domain (Kramer et al., 1998; Yu et al., 1998). APC3/Cdc27, APC6/Cdc16, APC7, and APC8/Cdc23 have a series of Cdk phosphorylation sites as well as tetratricopeptide (TPR) repeats, which are thought to be important for homophilic interactions between subunits (King et al., 1995; Irniger et al., 1995). Some of the APC/C subunits have unknown functions and no clear domain structure, such as APC12/Cdc26. Activity and specificity of the APC/C are regulated by phosphorylation (Kramer et al., 2000; Kraft et al., 2003) and by binding of cycle-specific activator proteins such as Cdc20/Fzy and Cdh1/Fzr (Dawson et al., 1993;

Sigrist and Lehner, 1997). APC/C^{Cdc20} is active during metaphase and anaphase, while APC/C^{Cdh1} is required during mitotic exit and to maintain cells in G_1 (reviewed in Fang et al., 1999).

Work in multiple organisms has confirmed the essential role of the APC/C in regulating mitotic progression and exit. In multicellular organisms, however, phenotypes with differing degrees of severity have been observed after loss of APC/C function. They range from early embryonic lethality in the murine APC2 knockout to late larval lethality in *Drosophila* APC2 null mutants to adult sterility in *C. elegans* APC2 RNAi knockdowns, *Drosophila* APC2 hypomorphic mutants, and *Arabidopsis* APC2 null mutants (Wirth et al., 2004; Kashevsky et al., 2002; Davis et al., 2002; Capron et al., 2003). One key to explaining this disparity comes from *Drosophila* where embryonic mitotic phenotypes are not observed in zygotic null mutants, but are observed in maternal hypomorphic mutants (Reed and Orr-Weaver, 1997). This observation suggests that the lack of strong early embryonic defects in *Drosophila* APC/C mutants is due to rescue by maternal protein. *Drosophila* develops rapidly and depends on maternal products for many of its embryonic divisions (reviewed in O'Farrell et al., 1989). In mice, the cell cycle is slow, in contrast, and zygotic transcription is observed early at the two-cell stage (reviewed in Schultz, 1993). Thus, the late-stage or tissue-specific mitotic defects observed in *Drosophila*, *C. elegans*, and *Arabidopsis* are most likely attributable to maternal rescue.

In a forward genetic screen for genes that regulate post-embryonic growth of the eye in the zebrafish, *Danio rerio*, we isolated a number of novel mutants with cell division defects in the eye (Wehman et al., 2005). Our study focused on a region of the

neural retina known as the ciliary marginal zone (CMZ) that is responsible for almost all retinal growth after embryogenesis (Marcus et al., 1999). The CMZ is located at the peripheral edge of the retina and is composed of a rare population of multipotent retinal stem cells and a much larger number of rapidly dividing progenitor cells with more restricted cell-fate competence (reviewed in Harris and Perron, 1998). The CMZ is arrayed such that the newly generated progenitors are located closest to the lens, near the putative stem-cell niche. Older progenitors are found more centrally, closer to the three layers of differentiated cells (reviewed in Link and Darland, 2001). This reproducible organization makes the CMZ an ideal system in which to carry out a screen for genes that regulate the proliferation of stem cells and progenitors.

Here we report the molecular identification of two mutants, *vij* and *gog*, found to have a reduced CMZ in the prior screen (Wehman et al., 2005). The corresponding genes encode subunits of the APC/C, Cdc16 and Cdc26. We show that, as in other organisms, the APC/C is required to regulate progression through mitosis and that mitotically arrested cells undergo apoptosis. We also show that these mutants have relatively late and tissue-specific defects, due to slow and uneven depletion of maternal stores. We reveal the remarkable stability of maternally supplied APC/C that persists through embryogenesis well into larval stages. Finally, we demonstrate that the APC/C is required to prevent re-entry into the cell cycle by quiescent cells.

RESULTS

The zebrafish genes gog and vij encode subunits of the APC/C

At larval stages, *gog* and *vij* mutant zebrafish have small eyes, but are otherwise the same size as their wild-type siblings (Figure 1A-C). The phenotype of *vij* (Figure 1C) is slightly stronger than that of *gog* (Figure 1B). The reduction in eye size is due to a decrease in proliferation from the CMZ (Wehman et al., 2005). The CMZ is greatly reduced by morphological criteria revealed by Nissl staining in *gog* and *vij* mutants (Figure 1H-J), but the central retina formed during embryogenesis is fully differentiated and supports visual responses (Wehman et al., 2005) (Figure 1D-F).

Positional cloning revealed that the *gog* and *vij* mutant phenotypes are caused by mutations in two subunits of the anaphase-promoting complex, Cdc26 and Cdc16, respectively (Supplemental Figure 1). In gog^{s109} mutants, a mutation in the 3' splice site at the beginning of the third exon of Cdc26 results in the use of a cryptic splice site two bases downstream. This aberrant splicing shifts the reading frame, causing five missense amino acids to be added before terminating prematurely, thus deleting two-thirds of Cdc26 protein (Figure 1L). In vij^{s514} and vij^{s517} mutants, nonsense mutations at amino acids 52 and 241 of Cdc16, respectively, also result in severe truncations that remove all or most of the TPR repeats (Figure 1M). These three mutations are predicted to cause null or severely hypomorphic alleles due to the extent of the protein that is lost.

If Cdc16 and Cdc26 belong to the same functional complex in zebrafish, we would expect the compound phenotype to be of similar strength to that of either *vij* or *gog* alone. To test this, we crossed gog^{s109} with vij^{s517}, identified double carriers using restriction enzyme-mediated genotyping, and scored the progeny of $gog^{s109/+}$, $vij^{s517/+}$

incrosses. We did not observe any phenotypes in transheterozygous $gog^{s1109/+}$, $vij^{s517/+}$ larvae. Larvae homozygous mutant for both *gog* and *vij* were indistinguishable from *vij* single mutants judged by their eye size (Figure 1G) and by the morphology of the peripheral retina (Figure 1K). The double-mutant phenotype provides genetic evidence that Cdc16 and Cdc26 are part of the same functional protein complex in zebrafish. Although our original screen (Wehman et al., 2005) found five other mutants with cell proliferation phenotypes similar to *gog* and *vij*, these other genes do not seem to encode additional subunits of the APC/C or either of the two known APC/C activators (Supplemental Table).

Loss of the APC/C in dividing retinal progenitors results in mitotic arrest and apoptosis

Given the known role of the APC/C in regulating mitosis, we asked whether there was evidence of a mitotic arrest in the CMZ of *gog* and *vij* mutants. We used phosphorylated histone H3 (PH3) as a marker for cells in late G_2 through M phase. In a typical wild-type retinal section, from one to three PH3-positive cells were observed in the CMZ on each side of the lens. These cells were typically scattered along the full extent of the CMZ from the lens to the photoreceptor layer (Figure 2B). In *gog* and *vij* retinal sections, we consistently observed an increased number of PH3-positive cells at the retinal margin (wild-type: 4±1; *vij*: 9±1, n=8, $p<0.005$), although the PH3-positive cells were typically clustered closer to the lens (Figure 2G). The two-fold increase in PH3-positive cells likely reflects a mitotic arrest in retinal progenitors. Alternatively, a greater number of cells might be cycling in *gog* and *vij* mutant retinas.

In order to rule out that more cells are dividing, we asked how many cells were in S phase using BrdU labeling. A complete cell cycle in the zebrafish CMZ at an early larval stage is thought to be six to eight hours (Li et al., 2000); so we incubated fish in BrdU for six hours to get an estimate of the number of cycling cells. When stained for BrdU incorporation at 4 dpf, we observed that the entire CMZ is labeled in wild-type larvae and that few cells with a differentiated morphology are labeled (Figure 2A). In *vij* and *gog* mutants, only a few cells (approximately 10-20% of wild-type) are BrdU-positive, reflecting a decrease in the number of cells passing through S phase (Figure 2F). These few BrdU-positive cells are in the same position, close to the lens, as the CMZ remnant revealed by Nissl staining (Figure 1H and 1I) and are therefore likely to be young retinal progenitors. We also see a consistent reduction in BrdU-labeled cells at later larval stages such as 6 dpf and 9 dpf (Figure 2M) (Wehman et al., 2005; data not shown). We interpret this reduction in the number of progenitor cells in the CMZ as a result of reduced division by these progenitors. In combination with the observed increase in the number of PH3-positive cells, this is consistent with a cell cycle arrest in the CMZ where each stem cell division results in a progenitor cell that cannot complete mitosis.

In order to further characterize this mitotic arrest, we compared the patterns of BrdU and PH3-labeled cells. In the wild-type CMZ, all PH3-positive cells are also BrdU-positive, and the PH3-positive population represents a small subset of BrdU-positive cells (Figure 2C). This pattern indicates that any cell in M phase has passed through S phase in the previous six hours. In *gog* and *vij* mutants, in contrast, most of the BrdU-positive cells in the CMZ are also PH3-positive (arrowhead in Figure 2H), but there is not a significant

increase in the total number of BrdU-positive, PH3-positive cells (wild-type: 4±1, *vij*: 5±1, n=8, p>0.1). More strikingly, we also regularly observed PH3-positive cells that were BrdU-negative in *gog* and *vij* mutants (*vij*: 4±1, n=8) (arrow in Figure 2H). We did not observe any PH3-positive, BrdU-negative cells in wild-type larvae (n=8, p<0.001). These PH3-positive, BrdU-negative progenitors must have completed S phase before the BrdU treatment (six hours earlier). Given that G_2 is thought to be relatively quick, it therefore seems likely that these progenitors have been stalled in M-phase for at least six hours. These cells were typically at a position in the CMZ most distant from the lens, where the oldest progenitors reside. This staining pattern is best explained by a mitotic arrest of retinal progenitors, which subsequently fail to undergo their characteristic amplifying divisions.

We then investigated what happened to the retinal progenitors after the mitotic stall. The stall could result in cell death, or arrested progenitors could eventually escape the prolonged mitosis and differentiate normally. To test this, we used TUNEL labeling as a marker of apoptosis. In wild-type retinal sections, we observed only three TUNEL-positive cells in the CMZ out of eight retinas examined (Figure 2D). In *gog* and *vij* mutant retinas, we observed a seven-fold increase in TUNEL-positive cells (*vij*: 3±1, n=8, p<0.001) (Figure 2I). This increase in TUNEL cells confirms that more cells are undergoing apoptosis in the CMZ of *gog* and *vij*. We then compared the TUNEL staining to the pattern of PH3 staining. In wild-type, the TUNEL-positive cells were in no consistent relationship to the PH3-positive cells (Figure 2E). In *gog* and *vij*, the TUNEL-positive cells were often located at a position in the CMZ most distant from the lens, where the oldest progenitors are found (Figure 2J). This location is similar to the position

of BrdU-negative PH3-positive progenitors that have been arrested for at least six hours (Figure 2H). This evidence demonstrates that upon loss of the APC/C, dividing retinal progenitors stall in mitosis for several hours and then die.

Slow depletion of maternal APC/C protein causes larval mitotic defects

The two APC/C mutants show no detectable abnormality in embryonic development and were grossly normal, save for their small eyes at larval stages. A possible explanation is that Cdc16 and Cdc26 are not essential for cell division at early developmental stages in zebrafish. Alternatively, these two APC/C subunits might be required for all mitotic divisions, but maternal deposits of RNA and/or protein might be sufficient for development to proceed through embryogenesis until the maternal contribution is exhausted. Consistent with the maternal-store depletion hypothesis, RNA in situ hybridization revealed that Cdc26 is expressed maternally in zebrafish. In fact, Cdc26 is expressed ubiquitously in the embryo and larva (data not shown). Unfortunately, protein distribution could not be determined, because antibodies directed against mammalian Cdc16 and Cdc26 do not recognize the corresponding zebrafish proteins (AMW, unpublished observations).

If the maternal depletion hypothesis is true, we should be able to delay the onset of the proliferation defect in the retina by increasing the initial amount of Cdc16 or Cdc26 present in the fertilized egg. Following injection of Cdc26 RNA at the one-cell stage, we observed that *gog* mutants had normally sized eyes at early larval stages (4-5 dpf; Figure 2N). This rescue was transient; *gog* mutants injected with Cdc26 RNA had smaller eyes at later larval stages (after 6 dpf) and their eyes remained intermediate in

size between wild-type larvae and uninjected *gog* mutants. Injection of Cdc26 RNA bearing the *s109* mutation was not able to rescue eye size at any stage.

To demonstrate rescue of cell division, we incubated the Cdc26-injected larvae and uninjected controls in BrdU for 18 hours starting at 3 dpf and fixed them at 5 dpf. In wild-type animals, this protocol labeled the CMZ and a large number of differentiated cells at the retinal periphery (Figure 2K, L). In *gog* mutants that had not been injected with Cdc26 RNA, we observed very few cells labeled with BrdU in the CMZ or among differentiated cells (Figure 2M). In contrast, in injected *gog* mutants, we observed a wild-type pattern of progenitors in the CMZ and differentiated cells labeled by BrdU (Figure 2N). Thus, complementation of the mutant with wild-type RNA efficiently rescued the cell proliferation phenotype. Furthermore, overexpression did not disrupt embryonic development in wild-type or mutant, suggesting that the cell cycle can proceed normally at widely varying levels of individual APC/C subunits.

When we further analyzed the BrdU-labeled sections, we discovered a large increase in PH3-labeled cells in injected mutants (Figure 2N) over uninjected wild-type (Figure 2K) and Cdc26 injected wild-type (Figure 2L). The majority of BrdU-positive progenitors in the CMZ are also PH3-positive in Cdc26-injected mutants except for the youngest progenitors close to the lens (Figure 2N). Given the transient nature of the rescue, this pattern of staining in injected mutants suggests that retinal progenitors rapidly arrest in mitosis while attempting to undergo their amplifying divisions. This is likely due to the level of APC/C falling below its critical threshold. Retinal stem cells, in contrast, divide rarely and may therefore be able to maintain sufficient levels of APC/C protein.

The APC/C is required for embryonic cell division

The previous results make it likely that maternal supply is sufficient for cell cycle progression during the embryonic stage of zebrafish development. To prove that the APC/C is necessary for mitosis in embryonic cells, we decided to use a dominant-negative approach. A truncated form of sea urchin Cyclin B (amino acids 13-110) was injected as protein into one blastomere at the 2-cell stage. This truncated protein is thought to out-compete endogenous APC/C targets when added in excess (Holloway et al., 1993). In over 50% of injected embryos, we observed a group of cells that were larger and had undergone fewer divisions (Figure 3B) when compared to uninjected embryos at the 32- to 128-cell stage (Figure 3A). In addition, these larger cells had often lost contacts with their neighbors (arrowhead in Figure 3B). At 1 dpf, most of the injected embryos were shrunken and malformed, if not dead (not shown). If we instead injected a control protein where the destruction box (D-box) motif had been mutated (13-110*), we observed no phenotype in injected embryos at any stage (Figure 3C). Mutation of the D-box prevents the APC/C from recognizing Cyclin B (Holloway et al., 1993). Thus, inhibition of maternal APC/C function results in an early and severe mitotic block. This is consistent with our interpretation that the larval defects in *gog* and *vij* mutants are due to the gradual loss of stable maternal protein.

APC/C loss disrupts the exocrine pancreas and other tissues

Given the essential function of the APC/C in dividing cells, we expected all tissues (not just the retina) to be affected by loss of Cdc16 and Cdc26. Both APC/C mutants, *gog* and *vij*, die at late larval stages around 12-14 dpf. We hypothesized that this

lethality could be due to a problem with food consumption or digestion because it coincides with the stage at which starved larvae typically die. To investigate the morphology of the gut, liver, and pancreas, we crossed *gog* and *vij* into a transgenic line expressing GFP in the endodermal organs (Field et al., 2003b).

We observed a striking phenotype in the exocrine pancreas. At 3 dpf, there is no difference between wild-type and *gog* or *vij* mutants in the size of the exocrine pancreas. Starting at 4 dpf in *gog* mutants, the exocrine pancreas becomes progressively shorter. By 5 dpf, the exocrine pancreas no longer reaches past the posterior extent of the swim bladder in *gog* mutants (Figure 4B). By 7 dpf, the exocrine pancreas is less than half its normal length (Figure 4D) and by 9 dpf, only the endocrine pancreas appears to remain (Figure 4F). In *vij* mutants, the phenotype appears earlier (3.5 dpf) than in *gog* and proceeds more rapidly. The exocrine pancreas is dramatically shorter by 4 dpf (Figure 4J) and apparently absent by 5 dpf (Figure 4L). We repeated our analysis with specific markers of the exocrine pancreas such as amylase (Figure 4O-P) and trypsin (not shown) and observed the same progressive shortening of the exocrine pancreas. Markers of the endocrine pancreas such as islet-1 and insulin appear normal at larval stages (AMW and PD Dong, unpublished observation). Given the role of the exocrine pancreas in producing digestive enzymes such as trypsin, these findings could explain the lethality of *gog* and *vij* mutants.

To confirm the maternal-store depletion hypothesis for this tissue, we rescued the exocrine pancreas phenotype by RNA injection. Injection of Cdc26 mRNA at the one cell stage was sufficient to fully rescue the pancreas in *gog* mutants at 9 dpf (Figure 4H). This result demonstrated that Cdc26 is unusually stable, because RNA rescue of a phenotype

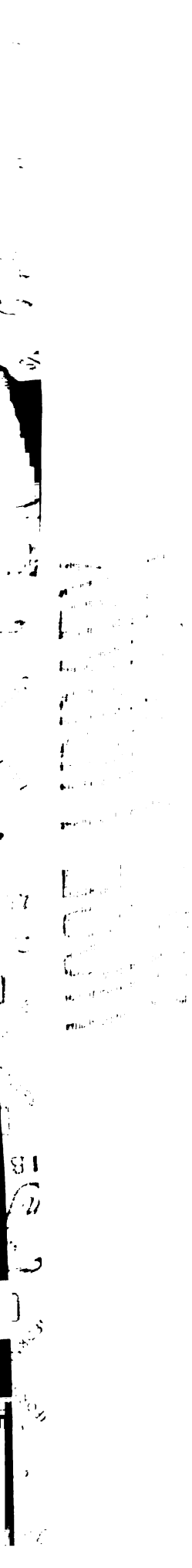

over a week after injection is atypical. Similarly, injection of Cdc16 mRNA into *vij* mutants at the one cell stage can delay the shortening of the pancreas by 1 or 2 days (Figure 4N). Although it seems clear that progressive loss of the exocrine pancreas is due to loss of the APC/C, it is unclear whether the apparent retraction is due to degeneration or another developmental defect.

Upon closer inspection, other tissues are also affected by loss of the APC/C. Most prominently, we observed a seven-fold increase in PH3-positive cells in the olfactory epithelium in *vij* mutants (not shown, wt: 2±1, *vij*: 16±1, n=8, $p<0.001$). Like the retina, the olfactory epithelium is still adding many cells at 4 dpf. We also investigated whether the cartilage in the head was altered using Alcian Green staining (Schilling and Kimmel, 1997). We discovered that the three posterior-most ceratobranchial arches are dramatically shorter in *vij* mutants at larval stages (Supplementary Figure 2). These are the last of the five ceratobranchial arches to form, first appearing at 64-68 hours post-fertilization (Schilling and Kimmel, 1997). These defects are consistent with the hypothesis that tissues that add many new cells at larval stages (such as the retina, olfactory epithelium, and late-forming branchial arches) are some of the first tissues affected by gradual depletion of the APC/C.

Loss of the APC/C in quiescent cells results in re-entry into mitosis

In addition to its role in mitosis, the APC/C is known to maintain cells in G_1 and prohibit immediate progression to the next S phase (reviewed in Peters, 2002). There is also recent evidence that removal of the APC/C in differentiated cells may cause them to leave G_0 and re-enter the cell cycle (Wirth et al., 2004; Almeida et al., 2005). If a mitotic

arrest were the only phenotype occurring in *gog* and *vij* mutants, we would observe a global decrease in BrdU-labeled cells, as we have seen in the retina. However, if loss of APC/C function also causes cells to re-enter the cell cycle from a quiescent state we would expect to see the exact opposite, an increase in BrdU-labeled cells.

In order to assay proliferation in many tissues simultaneously, we performed wholemount BrdU- and PH3- staining in *gog* and *vij* mutants after a 6-hr incubation in BrdU. This protocol is identical to the one used for our analysis of the retina where we observed an increase in the number of PH3-positive progenitors and a decrease in BrdU-positive progenitors (Figure 2). In contrast to the retina, we discovered a global increase in both BrdU- and PH3-positive cells in the mutant larvae at 4 dpf, a stage when there is normally a large amount of cell division occurring throughout the body (data not shown). This increase in BrdU incorporation is evident in most tissues, but is particularly striking in the tail and pectoral fins. In wild-type fins, new cells are mainly added at the distal edge, and few cells are observed to divide in the central and proximal parts (Figure 5B). In *vij* mutants, BrdU-positive cells are more dispersed at the distal edge of the fin, and more labeling is observed in the central and proximal portion of the fin (Figure 5D).

We repeated the wholemount BrdU- and PH3-staining in *gog* and *vij* mutants at 9 dpf, a stage when few cells should divide over a 6-hour period in wild-type larvae that have not been fed (Figure 5A, E). We observed a dramatic increase in the numbers of both BrdU-positive and PH3-positive cells in *vij* (Figure 5C) and *gog* (Figure 5G). In *gog* mutant larvae, there were twice as many BrdU-positive cells (wt: 149±14, *gog*: 342±66, n=5, $p<0.05$) and six times as many PH3-positive cells (wt: 37±5, *gog*: 225±25, n=5, $p<0.001$). Although *vij* mutants show the same widespread increase, *gog* mutants also

have a specific and dramatic increase in BrdU-positive cells evident in the gall bladder at 9 dpf (arrowhead in Figure 5G). These phenotypes are due to the slow and uneven depletion of APC/C in our mutants.

We finally asked whether there was a concomitant increase in TUNEL-positive apoptotic cells, above the background level of developmental apoptosis in wild-type larvae at 4 dpf (Figure 5I). We observed a global increase in TUNEL-positive cells in both *gog* (Figure 5K) and *vij* mutants (Figure 5M). This increase was especially striking in the pectoral fins of both mutants (Figure 5L & N), which also showed a substantial increase in proliferating cells (Figure 5D). As with all other phenotypes, the extent of apoptosis was more dramatic and began at an earlier stage in *vij* than *gog*.

The model that APC/C-depleted cells are unable to maintain G_0 and re-enter the cell cycle best explains the observation that both markers of proliferation, BrdU and PH3, are increased in most tissues. The observation that the increase of PH3-positive cells is always greater than the increase in BrdU-positive cells shows that the cells that inappropriately re-enter the cell cycle are also subject to prolonged mitotic arrest. Finally, the widespread increase in TUNEL-labeling suggests that mitotically arrested cells eventually die by programmed cell death.

DISCUSSION

In a forward-genetic screen for zebrafish mutants with arrested eye growth, we discovered seven loci required for proliferation of retinal progenitors (Wehman et al., 2005). By positional cloning we show here that two of the genes, *gog* and *vij*, encode Cdc26 and Cdc16, respectively, two subunits of the APC/C. Based on the protein sequence changes found in the single *gog* allele and the two *vij* alleles, we conclude that all three mutations have created (zygotic) null phenotypes. The phenotype of *gog/vij* double mutants is not stronger than that of either single mutant, suggesting that the two subunits work in the same functional protein complex in zebrafish cells as they do in other organisms.

Subsequent experiments using a dominant-negative inhibitor of the APC/C demonstrated that this protein complex is likely required for all mitotic divisions in the developing zebrafish. The early embryonic function of the APC/C is obscured in *gog* and *vij* mutants by maternal deposition of RNA and/or protein into the oocyte and by unusual stability of both Cdc16 and Cdc26 protein. Uneven depletion of the maternal store leads to tissue-specific defects, which are first apparent in the eye. Other tissues, such as the late-forming branchial arches and the olfactory epithelium are also affected, possibly due to rapid dilution of the maternal APC/C in frequently dividing cell types.

Prior to this study, several zebrafish mutants with defects in DNA replication and cell proliferation have been reported, especially from a large-scale mutagenesis screen using retroviral insertions (Amsterdam et al., 2004). Among these, mutations in MCM2 and MCM3 result in CMZ defects, similar to (although more pleiotropic than) the ones described here for *gog* and *vij* (Gross et al., 2005). Maternal stores may mask the

embryonic functions of MCM2 and MCM3, much in the same way as we have shown here for the APC/C. Therefore, we may find additional mutations in cell cycle regulators in our collection of CMZ mutants (Wehman et al., 2005), although the genetic map positions of the remaining five loci already exclude other APC/C components as candidate genes (Supplemental Table). In any case, the CMZ may provide an efficient system in which to discover genes universally involved in regulation of the vertebrate cell cycle that are supplied maternally and stable.

We used two cell-cycle markers to analyze the *gog* and *vij* phenotypes in more detail, the S phase tracker BrdU, which permanently labels cells that have undergone DNA replication during the incubation period, and the M phase marker PH3, which labels only those cells that are in late G2 or in mitosis at the time of fixation. We found that, in the retina, fewer progenitor cells in the marginal zone incorporate BrdU, and more of them are PH3-positive. This suggests that progenitors with insufficient quantities of Cdc16 or Cdc26 are arrested in mitosis (and therefore continue to label with PH3) and can no longer divide (and are therefore BrdU-negative). We could further show that mitotically arrested cells are eventually removed from the retina by programmed cell death. As a combined result of mitotic arrest and apoptosis, the eye fails to grow. Similar phenotypes were seen in the olfactory epithelium and the branchial arches. Injection of RNA encoding wild-type protein into mutant embryos at the one-cell stage was able to delay the cell proliferation defect by several days and transiently normalize organ growth. Overexpression of either Cdc16 or Cdc26 did not perturb embryogenesis, suggesting that the APC/C has a permissive function, does not have an inductive role in patterning the embryo, and may operate at widely varying concentrations of its individual subunits.

A different cell cycle phenotype was observed in several other tissues, including the tail and fins of both mutants and the gall bladder of *gog*. Here, regions that in wild-type contain mainly postmitotic cells now exhibit increased BrdU incorporation and increased PH3 labeling. We explain this finding by the known role of the APC/C in maintaining cells in G_1 by delaying entry into S phase (reviewed in Peters, 2002). If, in a quiescent cell, the APC/C levels drops below a certain threshold this cell may re-enter the cell cycle and begin DNA replication. The cells that re-enter the cell cycle proceed normally through G_2 but subsequently arrest in M phase, as evidenced in our experiments by the accumulation of PH3-labeled cells, which always exceeded the number of BrdU-positive cells. This phenomenon can explain why the exocrine pancreas not only stops growing, but also fails to maintain differentiated cells. In the retina, however, we did not observe ectopic BrdU-positive cells, which could mean that this tissue still maintains sufficient levels of APC/C protein. Alternatively, the reversal of the G_0 state after loss of APC/C may not occur in all cell types, such as retinal neurons. Cdk inhibitors are candidate factors that may work redundantly with the APC/C to keep these neurons in a postmitotic state (reviewed in Peters, 2002; see also Ohnuma and Harris, 2003).

Together, these experiments lead us to propose the following model of APC/C function in zebrafish. A functional APC/C is required for the correct progression from M phase through G_1 in dividing cells, as well as for maintenance of G_0 in quiescent and possibly differentiated cells (Figure 6A). When APC/C function is lost in a dividing cell, it results in mitotic arrest and apoptosis (Figure 6B). When APC/C function is lost in a quiescent or differentiated cell, it results in re-entry into the cell cycle, before the cell also arrests in mitosis and undergoes apoptosis (Figure 6B). To our knowledge, this report is

the first demonstration of the dual role of the APC/C in both dividing and quiescent cells in a living vertebrate. These two functions could only be revealed because of the maternal supply of Cdc16 and Cdc26 in zebrafish embryos. Maternal deposits of these proteins (1) rescue zebrafish APC/C mutants from an early mitotic arrest, (2) are stable, lasting through embryonic development and, in some tissues, to larval stages, and (3) are depleted unevenly among different cell types leading to tissue-specific phenotypes.

Although precedents exist for both APC/C functions discovered here, the field has not agreed on a unifying model of its role in multicellular organisms. In *Drosophila* APC2 null mutants, the imaginal discs are small and mitotic neural precursors arrest in mitosis and fail to differentiate, consistent with the APC/C functioning in dividing cells (Reed and Orr-Weaver, 1997). The authors propose, as we do here, that the absence of defects until larval stages is due to maternal rescue of embryonic mitotic divisions. They also report that in APC2 hypomorphic mutants, the germline is defective and embryos from mutant mothers display an early embryonic mitotic defect. These defects support the hypothesis that gradual loss of maternal APC/C leads to relatively late phenotypes. It is unclear whether these tissues are specifically affected or whether similar defects would be observed in other tissues if whole animal BrdU, PH3, or TUNEL assays were performed as in this study. Although *gog* and *vij* mutants were originally identified for having a slightly smaller eye, we discovered defects in every tissue we analyzed, i.e. retina, tectum, olfactory epithelium, pancreas, liver, branchial arches, pectoral fins, and tail. We believe this reflects a universal requirement for the APC/C in all cells. We explain the disparity between the early lethal phenotype of the APC2 mouse knockout and late larval defects in zebrafish and *Drosophila* APC/C mutants as a reflection of

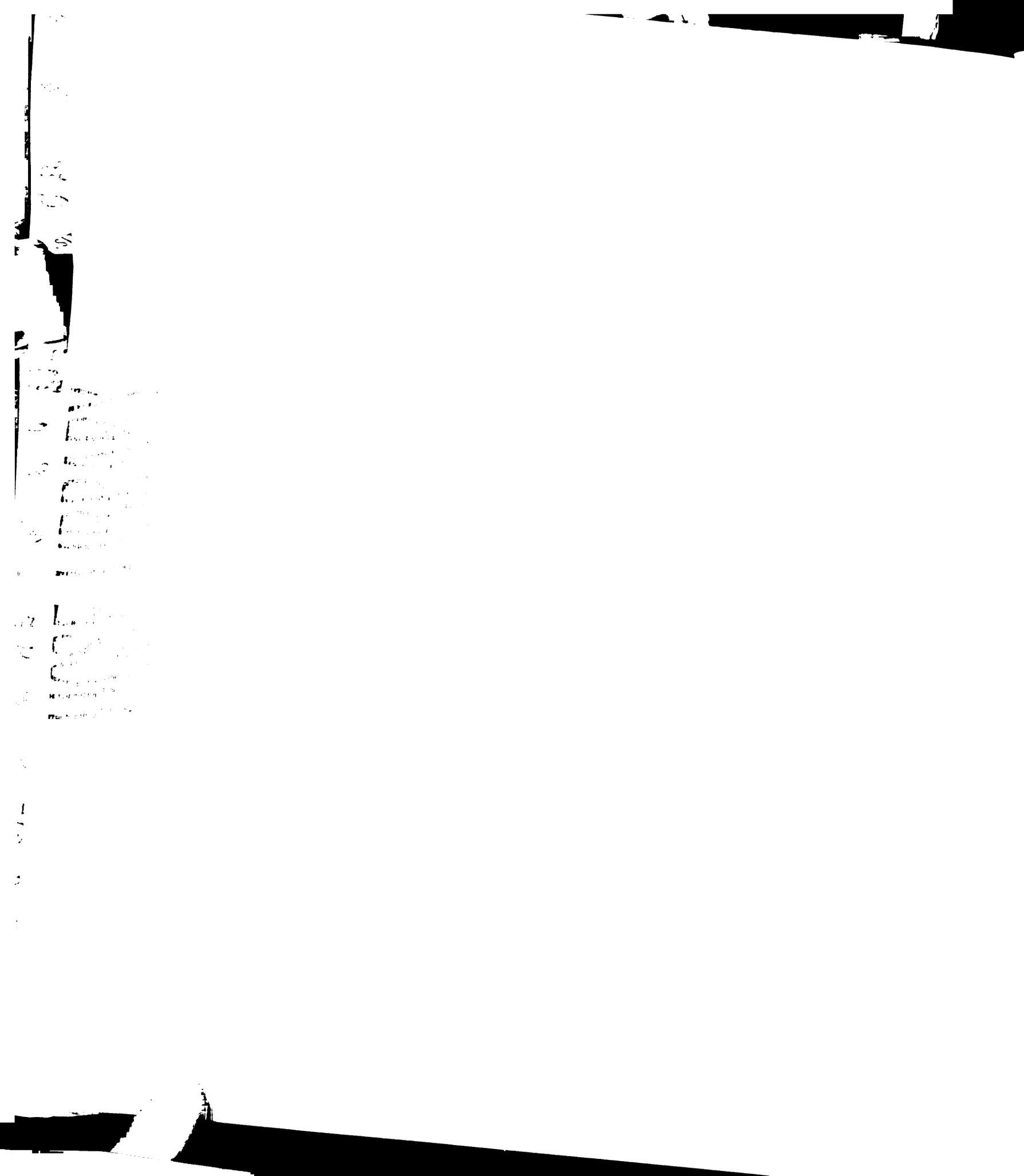

maternal loading. Zebrafish and *Drosophila* develop rapidly and depend on maternal products (reviewed in O'Farrell et al., 1989; Pelegri, 2003). In zebrafish, zygotic gene transcription begins at the thousand-cell stage (3-3.5 hours post-fertilization) (Kane et al., 1992). In contrast, the cell cycle is slow in mice and zygotic transcription is already observed at the two-cell stage (reviewed in Schultz, 1993).

Evidence for a role of the APC/C in maintaining the quiescent state (G_0) has been established by studies focusing on the response of individual tissues to loss of the APC/C, rather than a whole-organism view. In an elegant study making use of an inducible Cre-lox system, Wirth and colleagues analyzed the role of APC2 specifically in differentiated hepatocytes and discovered that, in the majority of livers analyzed, quiescent cells aberrantly re-entered the cell cycle before arresting in metaphase (Wirth et al., 2004). The small subset of livers that did not show spontaneous re-entry were still more responsive to mitogenic inducement, but it is not clear why these livers were phenotypically distinct after the same treatments in the same genetic background. A similar study in cultured rat neurons showed that loss of the APC/C activator Cdh1 in differentiated cells also resulted in re-entry into the cell cycle and eventually apoptosis (Almeida et al., 2005). The authors go on to show that these phenotypes are due to the accumulation of cyclin B, a major target of the APC/C. While these studies demonstrate that differentiated cells can re-enter the cell cycle upon loss of APC/C, we reveal that this principle can be applied to many tissues of the developing vertebrate.

While several studies propose that maternal APC/C is able to compensate for an absence of functional zygotic APC/C, few have remarked on its stability. In zebrafish, most maternal proteins are used up by 1 dpf (reviewed in Pelegri, 2003). Defects first

appear around 1 dpf in zebrafish Cyclin B1 mutants, as expected for an unstable, degraded protein that regulates the cell cycle (Amsterdam et al., 2004; AMW, unpublished observations). In *gog* and *vij* mutants, we observed a substantial number of cells continuing to divide after 9 dpf (Figure 5C, G). In addition, injection of RNA for Cdc26 at the one-cell stage rescued growth of the eye until at least 7 dpf and delayed retraction of the exocrine pancreas to at least 9.5 dpf. Clearly, Cdc26 protein must be unusually stable to function 9 days after it is produced. Subunits of the APC/C may be stabilized by their participation in a large protein complex, but they must also be able to function at low concentration, because considerable dilution will have occurred after 9 days of growth and division from one cell to the late larval stage. These aspects of the APC/C have been underappreciated by previous studies.

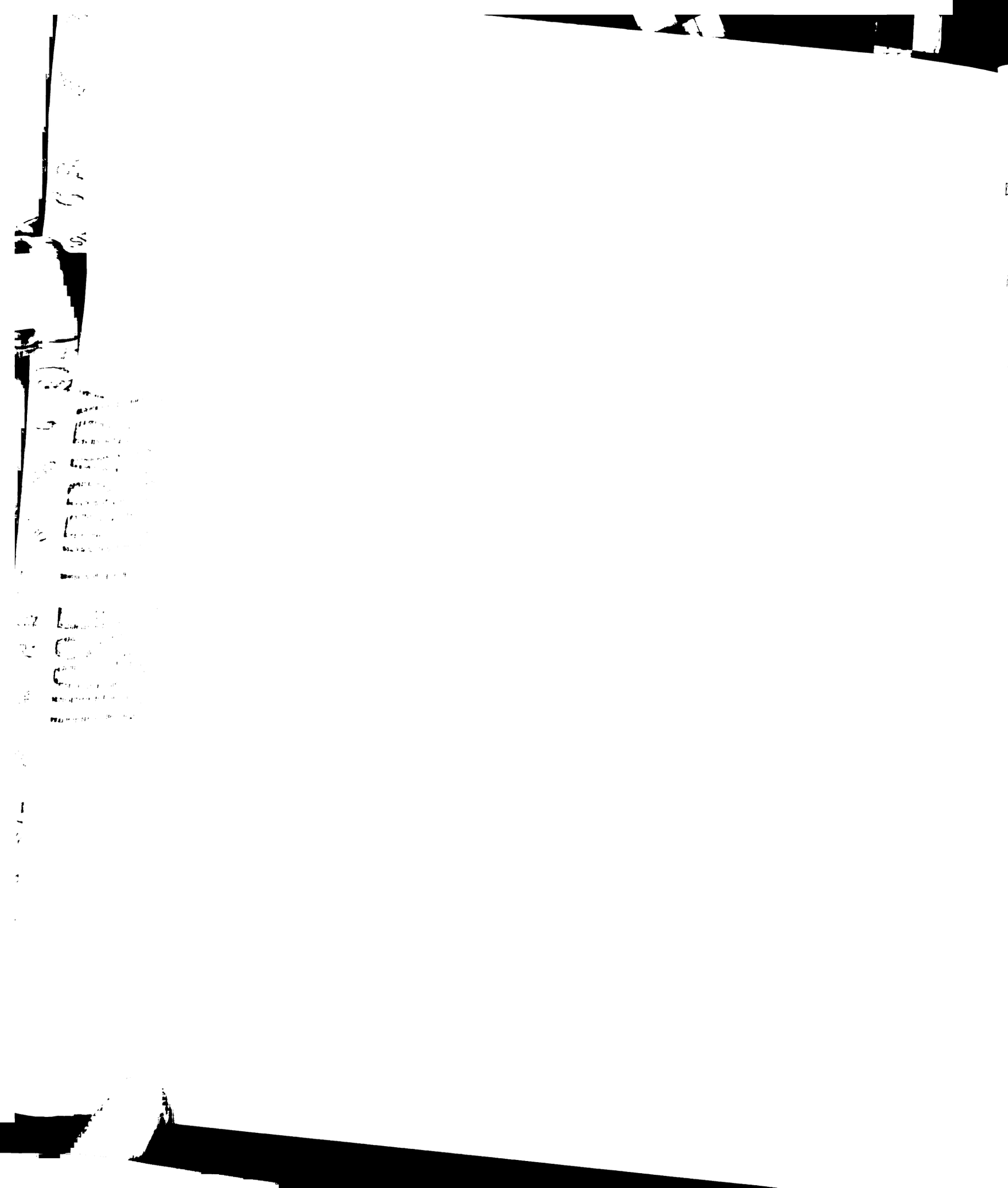

EXPERIMENTAL PROCEDURES

Injections

Fish were maintained as in Wehman et al. (2005). For rescue experiments, ~2 nl of 0.75 ng/nl Cdc26 (wild-type or *s109*) mRNA in Tris-EDTA (TE) were injected into the embryo at the one- to two-cell stage. For cyclin B experiments, we injected ~2 nl 165 mM protein (13-110 or 13-110*) in Tris-buffered saline (TBS) into one blastomere at the two-cell stage (gift of D. Morgan).

Positional cloning

Linkage mapping was performed as in Wehman et al. (2005). Zebrafish Cdc16 and Cdc26 were amplified using the following primers (Cdc16: CACAGGGGAACACTCACAAA and TCCAACACAGAGGACACGAT; Cdc26: CCCATGATTCCTTCTGCTCT and CACCGTTAACCAAAGCCATAA) and the sequences were deposited in Genbank (Accession# DQ356892 and DQ352177). These fragments were subcloned into pCS2+ for mRNA transcription using the mMessage mMachine kit (Ambion). To genotype gog^{s109}, the following primers and restriction enzyme were used: GTCCCTGCTCTCCCCTACTT, CCATTGTTCAGGATTAGCACT and MlyI (NEB). To genotype vij^{s517}, the following primers and restriction enzyme were used: GATGTTGTCGTCTCCCTTGCT, CTCAGCTCTACAAGGGTTCCTA, and BlpI (NEB).

Histology and immunohistochemistry

Nissl and DAPI staining and immunohistochemistry were performed on sections as in Wehman et al. (2005), except rabbit anti-phosphohistone H3 (1:500; Upstate). For wholemount immunohistochemistry, larvae were fixed in 4% paraformaldehyde (PFA) in phosphate-buffered saline (PBS), dehydrated in methanol and stored at –20°C. Larvae were then rehydrated and digested with 1 mg/mL collagenase for 2-3 h before staining. To examine cell proliferation, larvae were incubated in the thymidine analog 5-bromo-2-deoxyuridine (BrdU) at 2 mM in embryo medium for 6 h then returned to embryo medium without BrdU for at least 1 min before fixation. For Figure 2K-N, larvae were incubated in 2 mM BrdU for 18 h and returned to embryo medium for 36 h before fixation. To examine apoptotic cell death, wholemount TUNEL staining was performed as in Abdelilah et al. (1996) using the ApopTag kit (Chemicon) and TUNEL staining on sections was performed as in Kay et al. (2001) using the In Situ Cell Death Detection Kit (Roche). Alcian green staining was performed as in Schilling and Kimmel (1997). Gut staining was performed as in Field et al. (2003a), except rabbit anti-trypsin (1:100; Chemicon) and rabbit anti-amylase (1:100; Biomeda). All cell counts were performed on the most central retina section or on the whole larvae. Student's T-test was performed to assess the significance (*: $p<0.05$, **: $p<0.01$, ***: $p<0.001$).

ACKNOWLEDGEMENTS

The authors would like to thank Mary Matyskiela (Morgan lab, UCSF) for the gift of CycB protein as well as technical advice. David Morgan and David Toczyski generously provided advice. We thank Tobias Roeser for creation of *s161t*, the gut-GFP line. Wendy Staub, Victoria Kahn, Anna Reichardt, D. Ana Mrejeru, and Kerry Deere provided technical assistance. We would also like to thank Ellie Heckscher and members of the Baier lab for comments on the manuscript. AMW was funded by a dissertation fellowship from the AAUW Educational Foundation (American) and by an ARCS fellowship. Funding for this study was provided by NIH R01 EY13855 (HB).

REFERENCES

Abdelilah, S., Mountcastle-Shah, E., Harvey, M., Solnica-Krezel, L., Schier, A. F., Stemple, D. L., Malicki, J., Neuhauss, S. C., Zwartkruis, F., Stainier, D. Y., *et al.* (1996). Mutations affecting neural survival in the zebrafish Danio rerio. Development *123*, 217-227.

Almeida, A., Bolanos, J. P., and Moreno, S. (2005). Cdh1/Hct1-APC is essential for the survival of postmitotic neurons. J Neurosci *25*, 8115-8121.

Amsterdam, A., Nissen, R. M., Sun, Z., Swindell, E. C., Farrington, S., and Hopkins, N. (2004). Identification of 315 genes essential for early zebrafish development. Proc Natl Acad Sci U S A *101*, 12792-12797.

Capron, A., Serralbo, O., Fulop, K., Frugier, F., Parmentier, Y., Dong, A., Lecureuil, A., Guerche, P., Kondorosi, E., Scheres, B., and Genschik, P. (2003). The Arabidopsis anaphase-promoting complex or cyclosome: molecular and genetic characterization of the APC2 subunit. Plant Cell *15*, 2370-2382.

Castro, A., Bernis, C., Vigneron, S., Labbe, J. C., and Lorca, T. (2005). The anaphase-promoting complex: a key factor in the regulation of cell cycle. Oncogene *24*, 314-325.

Davis, E. S., Wille, L., Chestnut, B. A., Sadler, P. L., Shakes, D. C., and Golden, A. (2002). Multiple subunits of the Caenorhabditis elegans anaphase-promoting

complex are required for chromosome segregation during meiosis I. Genetics *160*, 805-813.

Dawson, I. A., Roth, S., Akam, M., and Artavanis-Tsakonas, S. (1993). Mutations of the fizzy locus cause metaphase arrest in Drosophila melanogaster embryos. Development *117*, 359-376.

Evans, T., Rosenthal, E. T., Youngblom, J., Distel, D., and Hunt, T. (1983). Cyclin: a protein specified by maternal mRNA in sea urchin eggs that is destroyed at each cleavage division. Cell *33*, 389-396.

Fang, G., Yu, H., and Kirschner, M. W. (1999). Control of mitotic transitions by the anaphase-promoting complex. Philos Trans R Soc Lond B Biol Sci *354*, 1583-1590.

Field, H. A., Dong, P. D., Beis, D., and Stainier, D. Y. (2003a). Formation of the digestive system in zebrafish. II. Pancreas morphogenesis. Dev Biol *261*, 197-208.

Field, H. A., Ober, E. A., Roeser, T., and Stainier, D. Y. (2003b). Formation of the digestive system in zebrafish. I. Liver morphogenesis. Dev Biol *253*, 279-290.

Glotzer, M., Murray, A. W., and Kirschner, M. W. (1991). Cyclin is degraded by the ubiquitin pathway. Nature *349*, 132-138.

Gross, J. M., Perkins, B. D., Amsterdam, A., Egana, A., Darland, T., Matsui, J. I., Sciascia, S., Hopkins, N., and Dowling, J. E. (2005). Identification of zebrafish insertional mutants with defects in visual system development and function. Genetics *170*, 245-261.

Harper, J. W., Burton, J. L., and Solomon, M. J. (2002). The anaphase-promoting complex: it's not just for mitosis any more. Genes Dev *16*, 2179-2206.

Harris, W. A., and Perron, M. (1998). Molecular recapitulation: the growth of the vertebrate retina. Int J Dev Biol *42*, 299-304.

Hershko, A., Ganoth, D., Pehrson, J., Palazzo, R. E., and Cohen, L. H. (1991). Methylated ubiquitin inhibits cyclin degradation in clam embryo extracts. J Biol Chem *266*, 16376-16379.

Holloway, S. L., Glotzer, M., King, R. W., and Murray, A. W. (1993). Anaphase is initiated by proteolysis rather than by the inactivation of maturation-promoting factor. Cell *73*, 1393-1402.

Irniger, S., Piatti, S., Michaelis, C., and Nasmyth, K. (1995). Genes involved in sister chromatid separation are needed for B-type cyclin proteolysis in budding yeast. Cell *81*, 269-278.

Kane, D. A., Warga, R. M., and Kimmel, C. B. (1992). Mitotic domains in the early embryo of the zebrafish. Nature *360*, 735-737.

Kashevsky, H., Wallace, J. A., Reed, B. H., Lai, C., Hayashi-Hagihara, A., and Orr-Weaver, T. L. (2002). The anaphase promoting complex/cyclosome is required during development for modified cell cycles. Proc Natl Acad Sci U S A *99*, 11217-11222.

Kay, J. N., Finger-Baier, K. C., Roeser, T., Staub, W., and Baier, H. (2001). Retinal ganglion cell genesis requires lakritz, a Zebrafish atonal Homolog. Neuron *30*, 725-736.

King, R. W., Peters, J. M., Tugendreich, S., Rolfe, M., Hieter, P., and Kirschner, M. W. (1995). A 20S complex containing CDC27 and CDC16 catalyzes the mitosis-specific conjugation of ubiquitin to cyclin B. Cell *81*, 279-288.

Kraft, C., Herzog, F., Gieffers, C., Mechtler, K., Hagting, A., Pines, J., and Peters, J. M. (2003). Mitotic regulation of the human anaphase-promoting complex by phosphorylation. Embo J *22*, 6598-6609.

Kramer, E. R., Scheuringer, N., Podtelejnikov, A. V., Mann, M., and Peters, J. M. (2000). Mitotic regulation of the APC activator proteins CDC20 and CDH1. Mol Biol Cell *11*, 1555-1569.

Kramer, K. M., Fesquet, D., Johnson, A. L., and Johnston, L. H. (1998). Budding yeast RSI1/APC2, a novel gene necessary for initiation of anaphase, encodes an APC subunit. Embo J *17*, 498-506.

Li, Z., Joseph, N. M., and Easter, S. S., Jr. (2000). The morphogenesis of the zebrafish eye, including a fate map of the optic vesicle. Dev Dyn *218*, 175-188.

Link, B. A., and Darland, T. (2001). Genetic analysis of initial and ongoing retinogenesis in the zebrafish: comparing the central neuroepithelium and marginal zone. Prog Brain Res *131*, 565-577.

Marcus, R. C., Delaney, C. L., and Easter, S. S., Jr. (1999). Neurogenesis in the visual system of embryonic and adult zebrafish (Danio rerio). off. Vis Neurosci *16*, 417-424.

Morgan, D. O. (1999). Regulation of the APC and the exit from mitosis. Nat Cell Biol *1*, E47-53.

Murray, A. W., and Kirschner, M. W. (1989). Cyclin synthesis drives the early embryonic cell cycle. Nature *339*, 275-280.

Murray, A. W., Solomon, M. J., and Kirschner, M. W. (1989). The role of cyclin synthesis and degradation in the control of maturation promoting factor activity. Nature *339*, 280-286.

O'Farrell, P. H., Edgar, B. A., Lakich, D., and Lehner, C. F. (1989). Directing cell division during development. Science *246*, 635-640.

Ohnuma, S., and Harris, W. A. (2003). Neurogenesis and the cell cycle. Neuron *40*, 199-208.

Pelegri, F. (2003). Maternal factors in zebrafish development. Dev Dyn *228*, 535-554.

Peters, J. M. (2002). The anaphase-promoting complex: proteolysis in mitosis and beyond. Mol Cell *9*, 931-943.

Reed, B. H., and Orr-Weaver, T. L. (1997). The Drosophila gene morula inhibits mitotic functions in the endo cell cycle and the mitotic cell cycle. Development *124*, 3543-3553.

Schilling, T. F., and Kimmel, C. B. (1997). Musculoskeletal patterning in the pharyngeal segments of the zebrafish embryo. Development *124*, 2945-2960.

Schultz, R. M. (1993). Regulation of zygotic gene activation in the mouse. Bioessays *15*, 531-538.

Sigrist, S. J., and Lehner, C. F. (1997). Drosophila fizzy-related down-regulates mitotic cyclins and is required for cell proliferation arrest and entry into endocycles. Cell *90*, 671-681.

Wehman, A. M., Staub, W., Meyers, J. R., Raymond, P. A., and Baier, H. (2005). Genetic dissection of the zebrafish retinal stem-cell compartment. Dev Biol *281*, 53-65.

Wirth, K. G., Ricci, R., Gimenez-Abian, J. F., Taghybeeglu, S., Kudo, N. R., Jochum, W., Vasseur-Cognet, M., and Nasmyth, K. (2004). Loss of the anaphase-promoting complex in quiescent cells causes unscheduled hepatocyte proliferation. Genes Dev *18*, 88-98.

Yu, H., Peters, J. M., King, R. W., Page, A. M., Hieter, P., and Kirschner, M. W. (1998). Identification of a cullin homology region in a subunit of the anaphase-promoting complex. Science *279*, 1219-1222.

Zachariae, W., and Nasmyth, K. (1999). Whose end is destruction: cell division and the anaphase-promoting complex. Genes Dev *13*, 2039-2058.

FIGURE LEGENDS

Figure 1. *gog* and *vij* mutants have small eyes and carry mutations in subunits of the APC/C.

A-C. Wholemount lateral views of live 4 dpf free-swimming larvae. In the gog^{s109} mutant **(B)**, the eyes are slightly smaller than in wild-type (A), but the animal appears otherwise **normal**. In the vij^{s517} mutant (C), the eyes are smaller, and the swimbladder is sometimes **uninflated**, but the animal appears relatively normal. **D-G.** Horizontal sections of 4 dpf **eyes** stained with Nissl (red), DAPI (blue), and PFA-induced autofluorescence (green). **H-K.** Magnified views of the anterior (nasal) ciliary marginal zone (CMZ) (between **arrows**) in Nissl-stained sections. The wild-type eye (D, H) displays the laminar structure **of** the retina and the Nissl-bright CMZ. In gog^{s109} (E, I) and vij^{s517} (F, J), as well as in **double** mutants gog^{s109}/vij^{s517} (G, K), the eyes are normal except for a greatly reduced **CMZ**. All sections are oriented anterior up. **L.** Structure of the wild-type and gog^{s109} **alleles** of Cdc26. The gog^{s109} allele is less than one-half wild-type length and ends with **five** amino acids not normally found in Cdc26 (purple box). **M.** Structure of the wild-type, vij^{s514}, and vij^{s517} alleles of Cdc16. Both *vij* alleles lose most of Cdc16 protein, **especially** the TPR repeats (dark green boxes). Scale bar in A-C, 500 μm. Scale bars in **D**-K, 50 μm. Scale bar in L-M, 50 amino acids.

Figure 2. Loss of the APC/C in dividing retinal progenitors results in mitotic arrest and apoptosis.

A-J. Horizontal sections of 4 dpf eyes stained for BrdU (green, after 6 h incubation) and PH3 (red). (A-C, F-H), or TUNEL (green) and PH3 (red) (D-E, I-J). Only the anterior (nasal) quarter of the eye is shown. Most or all cells in the wild-type CMZ are labeled with BrdU (A), a small subset of which is also PH3-positive (B, C, arrowhead). Paired arrowheads in A show the extent of the CMZ. Rarely, a TUNEL-positive cell is observed in wild-type (D, arrowhead), and this TUNEL-positive cell is also PH3-positive (E, arrowhead). In *vif*^{s517}, fewer cells are labeled with BrdU and the CMZ is smaller (F, between arrowheads). There are more PH3-positive cells in *vif*^{s517}, and they reside close to the lens (G, arrow and arrowhead). In *vif*^{s517}, most of the BrdU-positive cells are also PH3-positive (H, arrowheads), but there are also PH3-positive cells that are not BrdU-positive (H, arrow), which is not observed in wild-type. In *vif*^{s517} mutants, multiple TUNEL-positive cells are observed (I, arrowheads). Some of these TUNEL-positive cells are also PH3-positive cells (J, arrowheads). **K-N.** Horizontal sections of 5 dpf eyes stained for BrdU (green) and PH3 (red) one day after an 18-hour incubation in BrdU. Paired arrowheads mark the extent of the CMZ. In wild-type (K), many cells in the CMZ and differentiated cells are labeled with BrdU and a couple PH3-positive cells are observed. Wild-type larvae injected with Cdc26 RNA (L) are identical to uninjected wild-type larvae. In *gog*^{s109} mutants (M), very few cells are labeled with BrdU and PH3 and reside close to the lens. In *gog*^{s109} mutants injected with Cdc26 RNA (N), the number of BrdU-labeled cells is increased to wild-type levels, but most of the cells in the CMZ

also label with PH3. Sections are oriented anterior up. (O) Graph of cell counts (with standard error) from retinal sections as in A-J.

Figure 3. Inhibiting the APC/C results in a cell cycle defect at an early embryonic stage

Embryos were injected at the two-cell stage and photographed 2 hours later. **A.** In uninjected controls, the embryos has undergone 8 or 9 rounds of division and reached the 500- to 1000-cell stage by 3 hours post fertilization. **B.** In embryos injected with an N-terminal truncation of Cyclin B (amino acids 13-110), there are fewer cells and the cells are larger. Several cells on one side of the embryo appear to have lost contacts with their neighbors (arrowhead). **C.** Embryos injected with a mutated version of Cyclin B with two substitutions in the destruction box (13-110*) underwent normal division and had cells with regular size and morphology. Scale bar, 100 μm.

Figure 4. Loss of the APC/C results in retraction of the exocrine pancreas

A-N. Right side view of endodermal organs in the *s161t* GFP line. **O, P.** Right side view of larvae stained for amylase. Arrows in A-P mark the posterior extent of the exocrine pancreas. In wild-type (A), by 5 dpf, the exocrine pancreas (XP) extends from the endocrine pancreas (NP) past the posterior end of the swim bladder (SB). In gog^{s109} mutants (B), the exocrine pancreas no longer extends as far posteriorly as wild-type at 5 dpf. The morphology of the wild-type gut does not change dramatically between 5 and 7 dpf (C), while the exocrine pancreas extends less than half its normal length in gog^{s109} mutants (D). The exocrine pancreas continues to extend posterior to the swim bladder in wild-type larvae at 9 dpf (E). In gog^{s109} mutants, the exocrine pancreas is no longer

morphologically distinguishable from the endocrine pancreas at 9 dpf (F). In wild-type larvae injected with Cdc26 mRNA at the one cell stage, gut morphology is not perturbed at 9 dpf (G). In *gog*^{s109} mutants injected with Cdc26 mRNA, the progressive loss of the exocrine pancreas is rescued at 9 dpf (H). Wild-type (I, K) and *vij*^{s517} (J, L) gut at 4 dpf and 5 dpf. In *vij*^{s517} mutants, the exocrine pancreas has retracted to half its normal length by 4 dpf (J) and is no longer visible at 5 dpf (L). Injection of Cdc16 RNA does not alter gut development in wild-type larvae at 5 dpf (M), but temporarily rescues the exocrine pancreas in *vij*^{s517} (N). Amylase staining at 6 dpf confirms that the exocrine pancreas is reduced in *gog*^{s109} (O, P) Abbreviations: G: Gall Bladder, I: Intestine, L: Liver, NP: Endocrine Pancreas, SB: Swim bladder, XP: Exocrine pancreas. Scale bar, 500 μm.

Figure 5. Loss of the APC/C in dividing and quiescent cells results in mitotic arrest and apoptosis.

A-H. Larvae were stained as wholemounts for BrdU (green) and PH3 (red) immediately after a 6-hour incubation in BrdU. Ventral and lateral views of 9 dpf larvae show that few cells divide in unfed wild-type (A, E), whereas many cells are BrdU- and PH3-positive in *vij*^{s514} (C) and *gog*^{s109} (G). In *gog*^{s109} , the gall bladder (arrowhead) shows an especially striking increase in dividing cells (G). Graph of BrdU (F) and PH3 (H) cell counts (with standard error) from A, C, E, G. Pectoral fin dissection shows that quiescent cells are re-entering the cell cycle at 4 dpf. In wild-type, division is mostly restricted to the distal edge of the fin (C, double arrow). In *vij*^{s517} mutants, more cells divide and the division is more dispersed (D, double arrow). **I-N.** PTU-treated larvae stained for TUNEL (purple) at 4 dpf. Lateral views of wholemount larvae (I, K, N) and dissected pectoral fins (J, L,

N) with the indicated genotype are shown. There is a developmental background of apoptosis in wild-type larvae (I), although dying cells are rarely observed in the pectoral fin (J, arrowhead). There is a significant increase in apoptotic cells in gog^{s109} mutants, especially in the head and pectoral fin (K, purple box, L). Many cells are dying in vij^{s517} mutants, especially in the head, pectoral fin and tail (M, purple box, N). Fins are oriented proximal to the left, distal to the right. Scale bar in B, 100 μm. Scale bar in I, 500 μm.

Figure 6. Model of cell cycle progression with and without APC/C function.

A. In normal cells, the mitotic cell cycle progresses from G_1, when cells prepare to replicate their genome, to S, when DNA synthesis occurs. After duplicating each chromosome, they then progress to G_2, when they prepare for M. Finally, in M, the cells line up their chromosomes and the mitotic spindle ensures that each daughter will receive one copy of the genome before cytokinesis occurs. The daughters then have the choice to re-enter the cell cycle (G_1) or to exit the cell cycle and enter into G_0. Quiescent cells in G_0 typically go on to differentiate. APC/C^{Cdc20} is required for progression from metaphase to anaphase. APC/C^{Cdh1} function is required for correct regulation of mitotic exit and to maintain cells in G_0 and G_1. **B.** In cells that lack functional APC/C protein, all phases of the cell cycle are affected except S and G_2. Cells that are in G_1 are hurried into S and cells that are in G_0, whether quiescent or differentiated, re-enter G_1. After completing S and G_2, cells line up their chromosomes in metaphase, but then arrest. Sister chromatid separation does not occur and the cell is trapped in M for hours. Finally, the arrested cell undergoes apoptosis.

SUPPLEMENTARY INFORMATION:

Supplemental Figure 1. Positional cloning of *gog* and *vij*

(A) The *gog* interval was narrowed down to a 0.1 cM region (roughly 70 kb) on Chromosome 5 using a panel of 2035 mutant larvae (4070 meioses). This region contained at least two genes, a copper uptake protein (fd46a06 or AY077715) and Cdc26. The splice site mutation in Cdc26 and gog^{s109} show perfect linkage. (B) The *vij* interval was 0.5 cM (roughly 350 kb) on Chromosome 9 using a panel of 625 mutant larvae (1250 meioses). This region contained multiple genes, including Cdc16. All recombinants were lost at the nonsense mutation in Cdc16 in vij^{s517}.

Supplemental Figure 2. The branchial arches are shortened in *vij* mutants

Ventral views of larvae stained for cartilage using Alcian green at 6 dpf. The five ceratobranchial arches are traced in yellow. (A) In wild-type larvae, all five arches extend from the midline laterally to a position even with the jaw joint. (B) In gog^{s109} mutants, the cartilage of the arches is unaffected and they extend the normal length. (C) In vij^{s517} mutants, the last three ceratobranchial arches are clearly shorter and extend laterally only half the normal length.

Figure 1

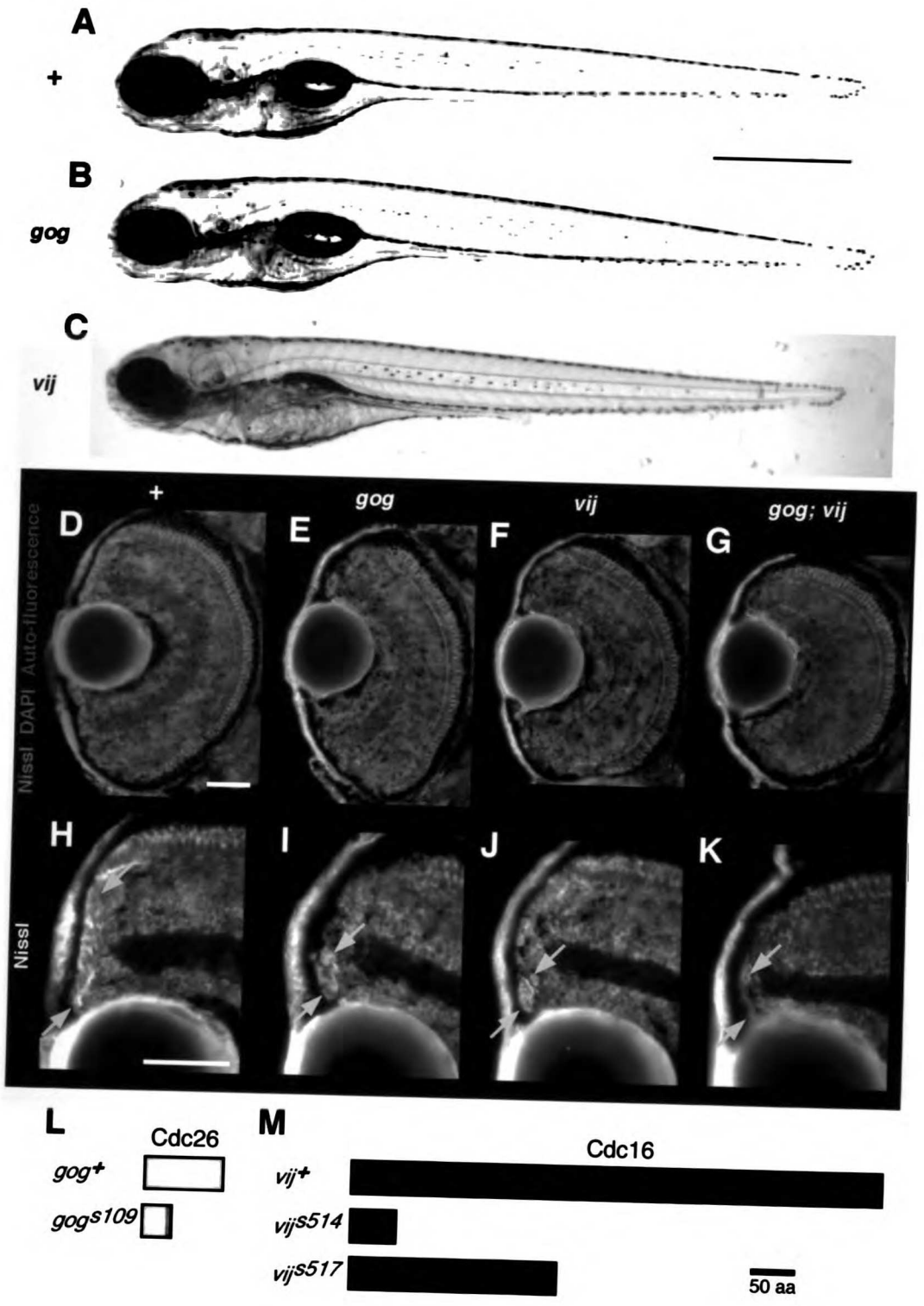
A
+
B
gog
C
vij
+
gog
vij
gog; vij
D
E
F
G
Nissl DAPI Auto-fluorescence
H
I
J
K
Nissl
L
Cdc26
gog+
gogs109
M
Cdc16
vij+
vijs514
vijs517
50 aa

Figure 2

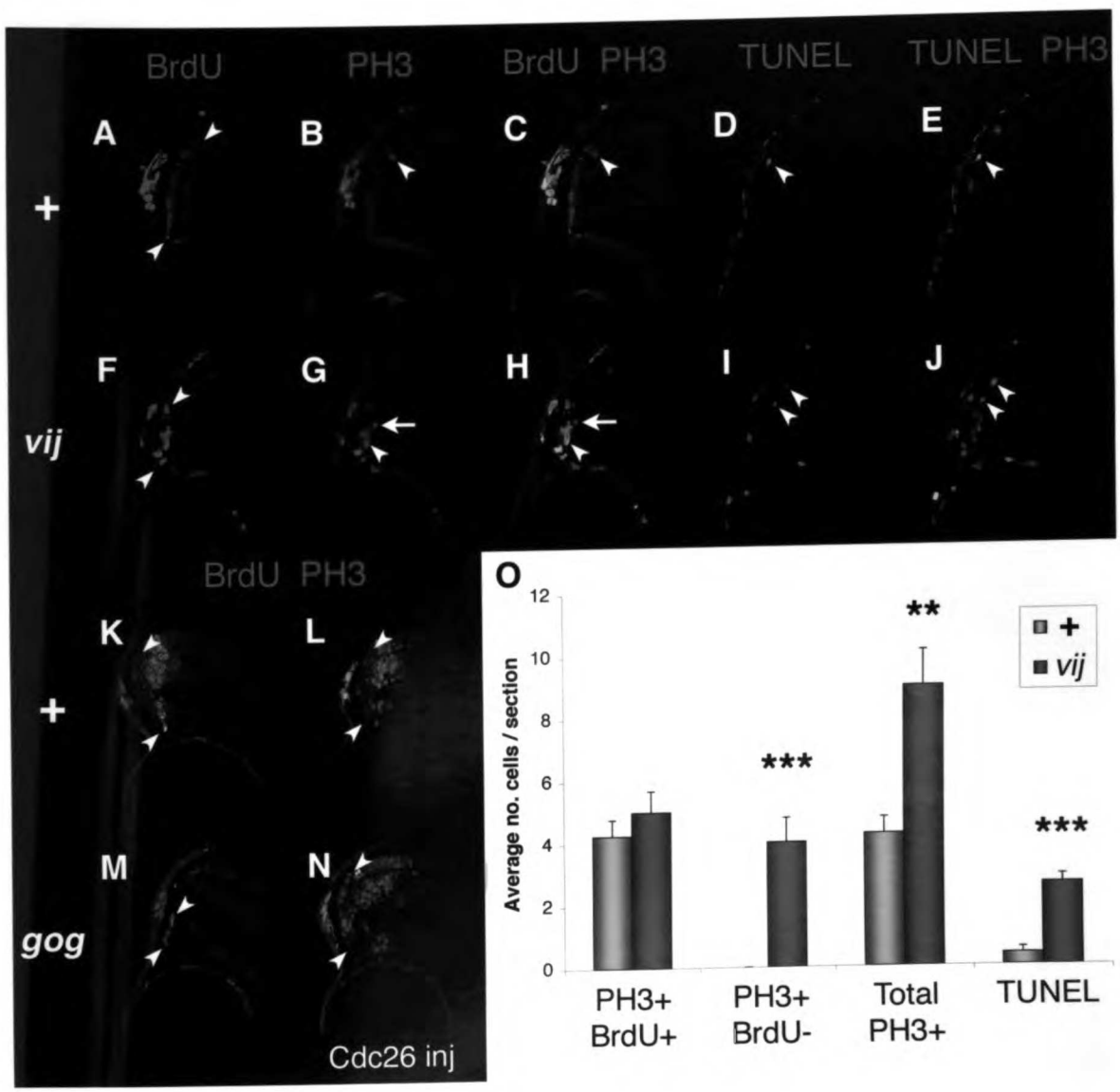
BrdU
PH3
BrdU PH3
TUNEL
TUNEL PH3
A
B
C
D
E
+
F
G
H
I
J
vij
BrdU PH3
K
L
+
M
N
gog
Cdc26 inj
O
Average no. cells / section
12
10
8
6
4
2
0
**
***
***
+
vij
PH3+ BrdU+
PH3+ BrdU-
Total PH3+
TUNEL

Figure 3

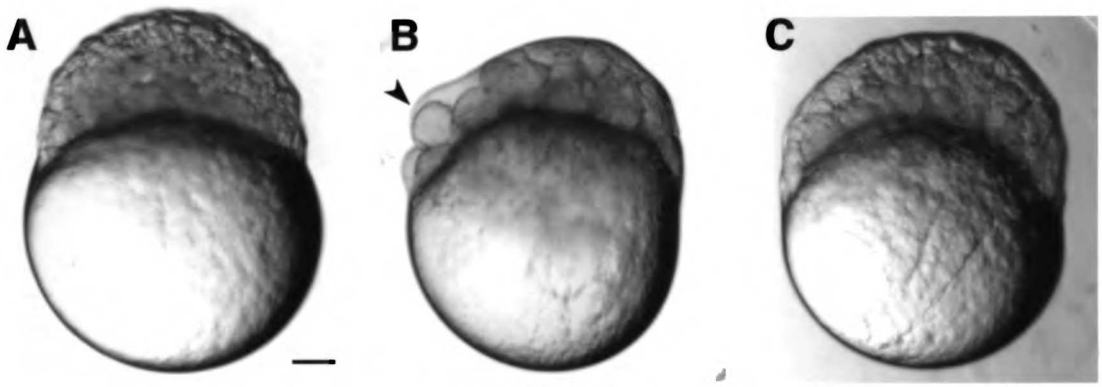

Figure 4

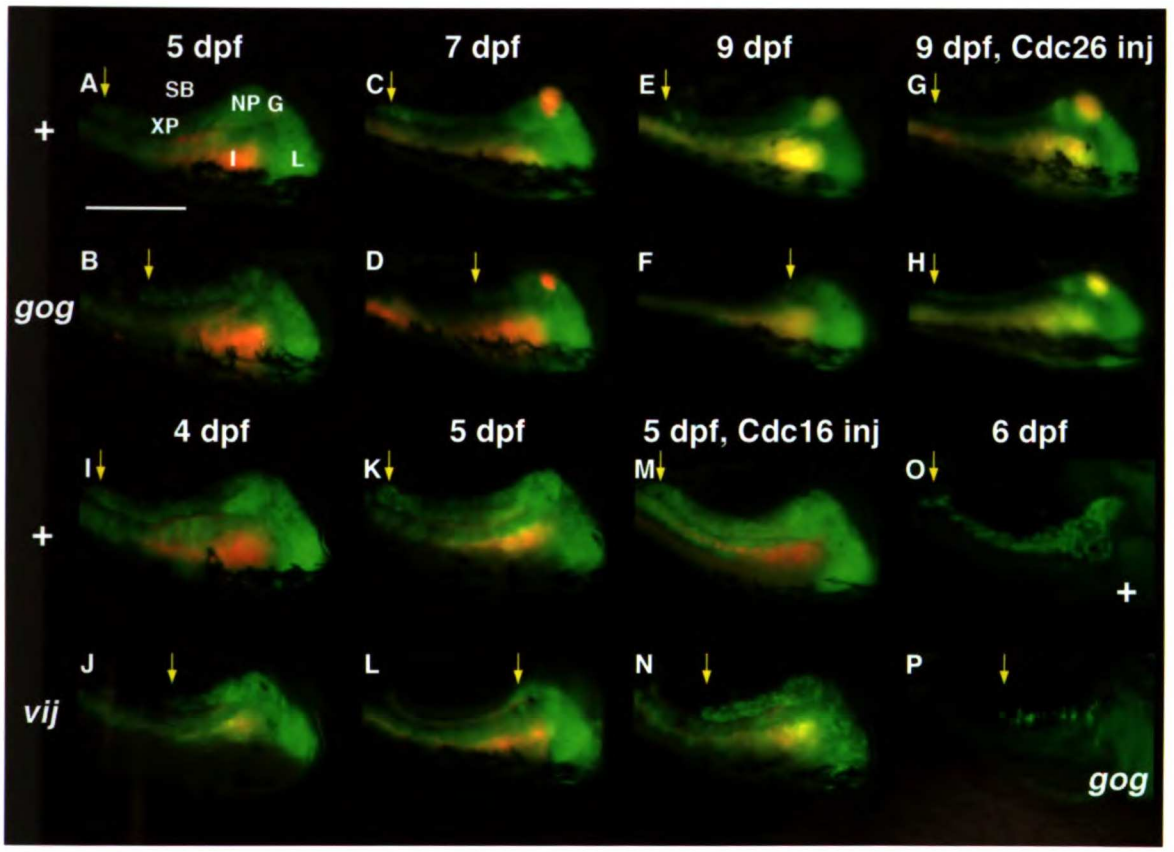
5 dpf
7 dpf
9 dpf
9 dpf, Cdc26 inj
A
SB
NP G
XP
I
L
C
E
G
+
B
D
F
H
gog
4 dpf
5 dpf
5 dpf, Cdc16 inj
6 dpf
I
K
M
O
+
J
L
N
P
vij
gog

Figure 5

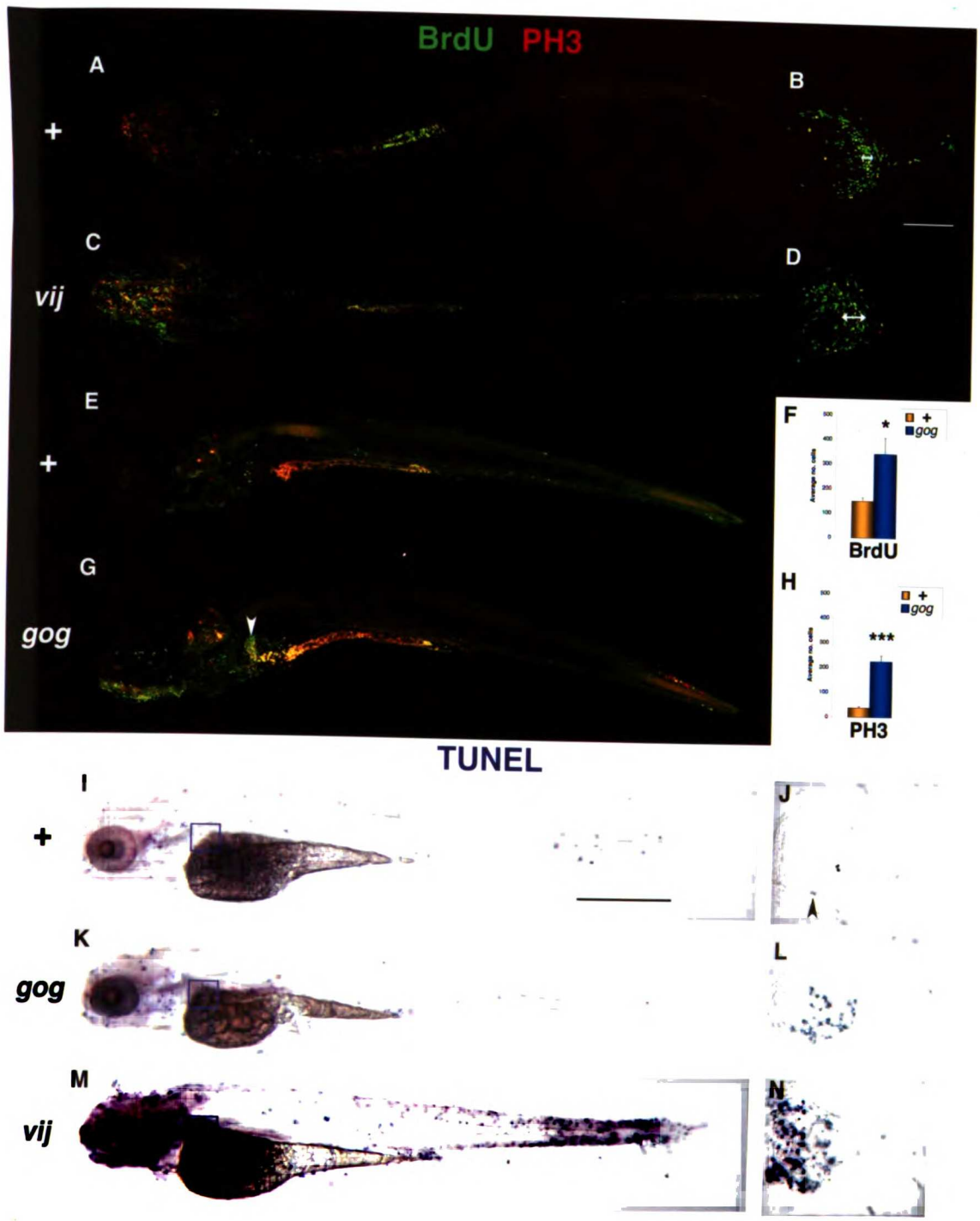
BrdU PH3
A
+
B
C
vij
D
E
+
F
+
gog
*
BrdU
G
gog
H
+
gog
***
PH3
TUNEL
I
+
J
K
gog
L
M
vij
N

Figure 6

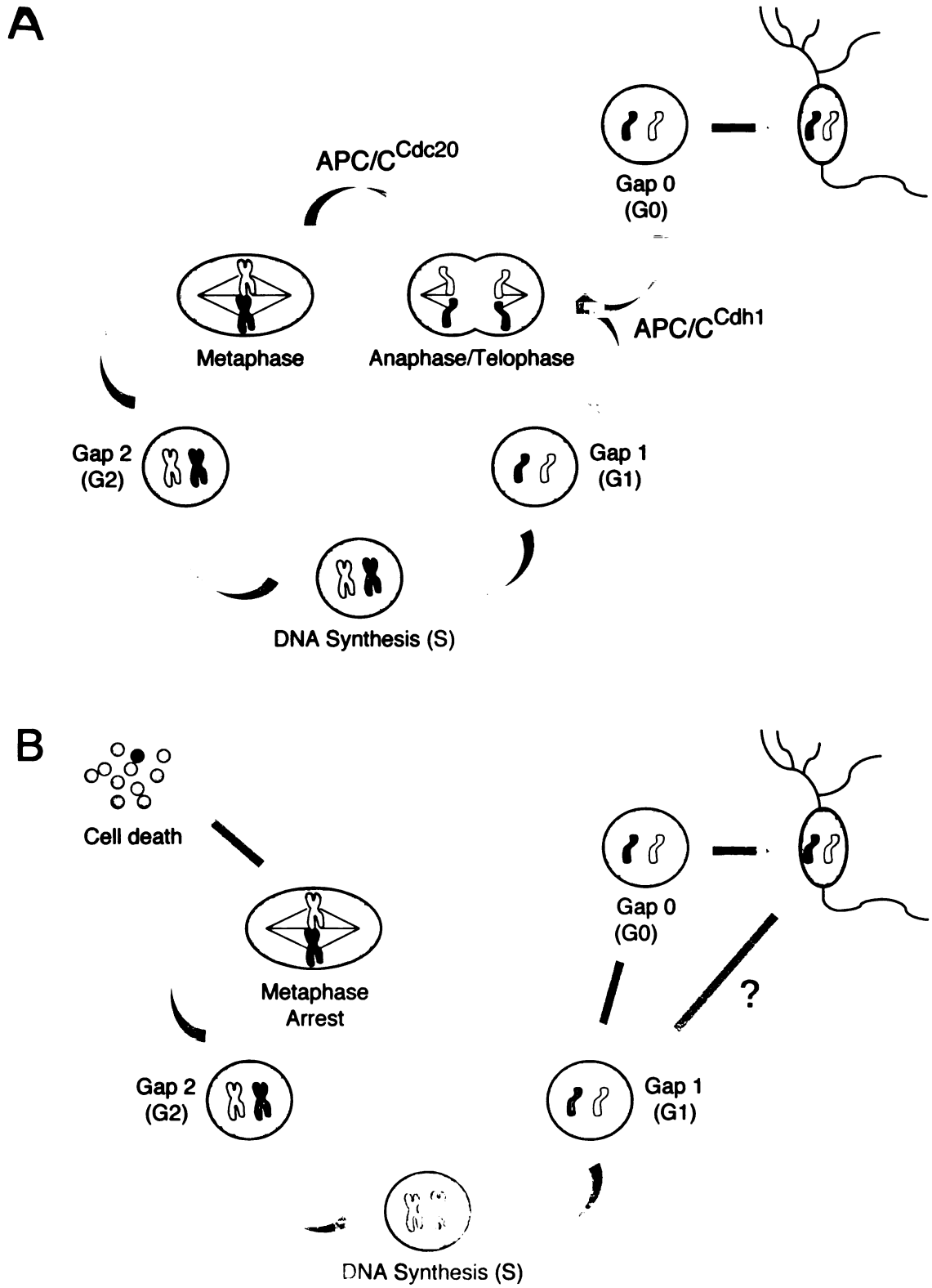
A
APC/C^Cdc20
Gap 0
(G0)
Metaphase
Anaphase/Telophase
APC/C^Cdh1
Gap 2
(G2)
Gap 1
(G1)
DNA Synthesis (S)
B
Cell death
Metaphase
Arrest
Gap 0
(G0)
?
Gap 2
(G2)
Gap 1
(G1)
DNA Synthesis (S)

Supplemental Table 1

Map positions of zebrafish APC/C subunits and activators

Subunit	Chromosome	Position (cM)
APC1/Tsg24	13	51-57
APC2	5	58-60
APC3/Cdc27	3	59-61
APC4	20	66-68
APC5	8	61-63
APC6/Cdc16	9	54-56
APC7	8	39-43
APC8/Cdc23	21	42-49
APC9	N/A	N/A
APC10/Doc1	16 or 23	LG16@79cM or LG 23@54cM
APC11	14	49-51
APC12/Cdc26	5	61-61
APC13/Swm1	21	38-41
APC15	21	36-38
Activator	**Chromosome**	**Position (cM)**
Cdc20/Fzy	2	39-41
Cdh1/Fzr	5	61-64

Positions are based on the MGH microsatellite map current as of publishing

Supplemental Figure 1

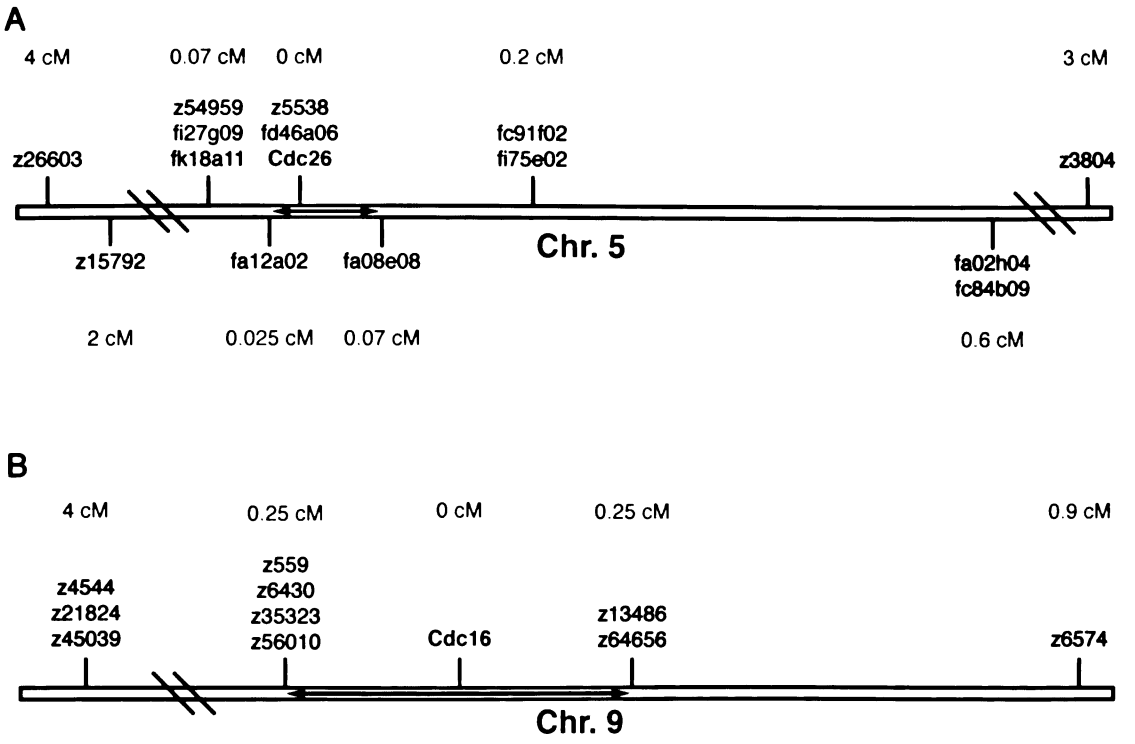

Supplemental Figure 2

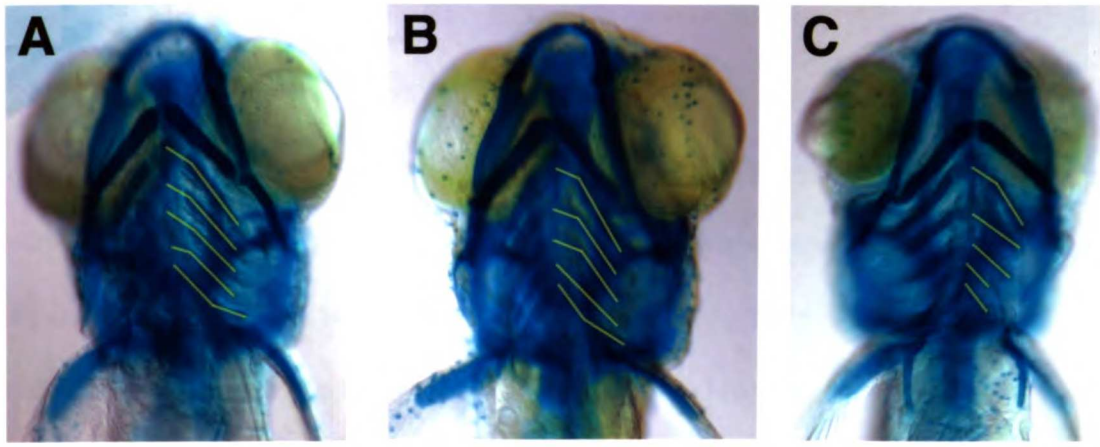

CONCLUSION

Do embryonic and adult stem cells use the same genes for their regulation?

In the end, a study designed to elucidate the mechanisms by which post-embryonic stem cells regulate proliferation and quiescence became research into the regulation of how all cells divide or stay quiescent. In hindsight, this result may not be surprising given the extent of maternal deposition in zebrafish. Rather, it illustrates that post-embryonic stem cells use many of the same mechanisms as embryonic stem cells to regulate their division.

Although the research described forms two complete stories, the larger project we initiated remains unfinished. For 16 more mutants, the mutated gene has not been identified. It is unclear whether they will all be genes that are required for cell division or survival, but where this requirement is masked during embryogenesis by maternal contribution. It remains possible that some will be genes that are specifically expressed in stem cells and are required for their maintenance. In either case, the complete set will reveal whether post-embryonic stem cells use novel mechanisms for their regulation or whether they use exactly the same toolbox as embryonic stem cells.

To date, the evidence is strongly in favor of post-embryonic stem cells simply recapitulating embryonic development. Jeff Gross and colleagues published a series of zebrafish insertional mutants with visual system defects, including those with marginal zone defects similar to those reported in Chapter 1 (Gross et al., 2005). These mutants also have similar gut and jaw defects to the mutants reported here. The insertions that affected the marginal zone were mostly in genes involved in DNA replication, but also

included a gene involved in post-translational modification of mRNA and two novel genes of unknown function. Based on our current knowledge of these genes, they are unlikely to have a unique function in post-embryonic retinal stem cells or their progenitor daughters.

One flaw of the zebrafish CMZ as a system to study stem cells is that it is not yet possible to prospectively identify the retinal stem cell. Our screen was based on following the progenitors as a functional read-out of the stem cell. No unique markers exist for the retinal stem cell, unlike the germline stem cell. Once a marker is found, it will be interesting to compare the results of a stem cell marker-based screen with our screen to see if one method is more successful at discovering genes that specifically regulate or are specifically expressed in post-embryonic stem cells.

We also do not know what cells, if any, act as a niche for the retinal stem cell in the CMZ. It has been reported that fish retinal stem cells do not require a supportive environment, because they can be cultured long-term *in vitro* without any growth factors in the media (Vince Tropepe and Derek van der Kooy, personal communication). No other stem cell can be maintained when taken out of its niche and cultured without specific growth factors. If there is, in fact, no retinal stem cell niche, then it is not surprising that the genes we found regulate the fundamental and defining characteristics of stem cells such as cell division.

One of the post-embryonic stem cell populations most amenable to genetic studies is the *Drosophila* germline stem cell (GSC). Using this system, gene pathways have been defined that regulate the interactions between a stem cell and its niche. For example, JAK/STAT signaling is required for self-renewal of GSCs in *Drosophila* (Kiger et al.,

2001; Tulina and Matunis, 2001). The hub cell in male testes expresses Upd, the ligand that activates JAK/STAT signaling in the GSC, such that only the GSCs close to the hub receive the self-renewal signal (Harrison et al., 1998). To date, the downstream transcriptional targets of STAT that are important for stem cell maintenance are unknown. Other mechanisms used to regulate GSC maintenance include polarized adhesion to the niche and mitotic spindle orientation (reviewed in Yamashita et al., 2005). For example, mutation of centrosome components in the germline results in an increase in stem cells due to the loss of properly oriented divisions (Yamashita et al., 2003). These mechanisms ensure that GSCs close to the niche retain their stem cell character, but as they move away from the niche, they are able to divide multiple times and differentiate into germ cells.

It should be noted, however, that although these functions are clearly important for the regulation of GSCs, neither of the example genes are used exclusively in post-embryonic stem cells. JAK/STAT signaling is also required to maintain the pluripotency of murine embryonic stem cells (reviewed in Eckfeldt et al., 2005) as well as its roles in eye development, the immune response, and segmentation in *Drosophila* (reviewed in Zeidler et al., 2000; Hou et al., 2002). The centrosome component used by Yamashita and colleagues is actually the result of an apparent duplication where one copy is expressed only in the germline and the other copy is expressed in somatic cells. Therefore, while these studies in the Drosophila germline have discovered several important mechanisms for regulating post-embryonic stem cells, they have not discovered genes that are solely dedicated to post-embryonic stem cell regulation.

Another well-defined post-embryonic stem cell population is the hematopoietic stem cell (HSC), which has long been the focus of considerable research. Two of the genes vital to long-term maintenance of HSC survival are Bmi1 and p21/Cdkn1a. Bmi1 is a Polycomb family transcriptional repressor that is thought to keep levels of differentiated genes low so that HSCs can maintain their pluripotency (Lessard et al., 1998). Cdkn1a is a cell-cycle inhibitor and is thought to help maintain HSCs in a quiescent state (Cheng et al., 2000). Again, these genes are instructive in describing the mechanisms that stem cells use to regulate, but not as unique markers for stem cells or unique functions in stem cells.

In an effort to reveal the genes that are enriched in stem cells, three studies compared the transcriptional profile of a few types of embryonic and adult stem cells with each other, their progenitor daughters and/or their differentiated progeny (Ivanova et al., 2002; Ramalho-Santos et al., 2002; Fortunel et al., 2003). Only one gene, integrin-α6, was enriched in all stem cell types in all three studies (although this may reflect technical differences rather than insight into stem cells). That all stem cells have high levels of integrin-α6 could reveal that one universal characteristic of stem cells is their desire to respond to or communicate with their environment.

Taken together, these studies suggest that post-embryonic stem cells do not have a dedicated set of regulatory genes. It seems more likely that post-embryonic stem cells use mechanisms similar to those used by embryonic stem cells as well as many other cell types. Therefore, the only way to study the mechanisms used by post-embryonic stem cells is to develop systems where you can alter gene function in only a subset of cells. Well-characterized genetic tools exist to target the germline in *Drosophila*. HSCs can be cultured and transplanted, allowing specific manipulation of HSCs. In zebrafish, maternal

stores allow embryogenesis to proceed normally such that genes required in post-embryonic stem cells can be isolated, as described in this work.

The pan-retinal stem cell and the APC/C

In Chapter 1, we proposed a model describing the cell types in which we expected our three subclasses of genes to act. This model was based on genetic epistasis experiments using our mutants. We indicated that Class I-B genes acted in the pan-retinal stem cell that was capable of creating both RPE progenitors and neuroretinal stem cells in the CMZ. Class I-A genes were thought to act in these neuroretinal stem cells or in their early progenitor daughters in the CMZ. We believed that Class II genes function in older, more restricted progenitors in the CMZ that will soon differentiate to give rise to the various neuronal and glial cell types in the retina.

How do these predictions stand up, now that the molecular identity of the Class I-A mutant used to create this hierarchy is known? As described in Chapter 2, *gog* is Cdc26, a subunit of the anaphase-promoting complex (APC/C). Cdc26 is predicted to be required for all mitotic division during zebrafish development, but maternally provided Cdc26 obscures this requirement in many cells during embryogenesis and larval development. For Class II mutants, the interpretation of the Class I-A, Class II double mutant is unchanged. When the neuroretinal stem cell or early progenitors are arrested in mitosis and die (as in *gog*), the later progenitors are not made. If there are no later progenitors, then they cannot amass to create an expanded CMZ (the Class II phenotype). Therefore, our original model correctly predicted the reason behind the observed epistatic relationship.

The epistatic relationship observed between *gog* and the Class I-B mutant, *kes*, is more challenging to justify in light of *gog*'s identity. It is surprising that any tissues would be expanded in the absence of Cdc26. There are several possible explanations for the observation that the Class I-A, Class I-B double mutant looks like *kes* with an expanded peripheral RPE.

The first two possibilities depend on postulating intrinsic differences between the division patterns of RPE progenitors and retinal progenitors. Stem cells are known to divide infrequently and could therefore be able to hoard their stores of Cdc26. This is supported by the observation that rare cells continue to divide in the CMZ remnant at 9 dpf in *gog* and *vij* (as reported in Chapter 2). If the RPE progenitor differentiates soon after its creation without multiple additional divisions, it may still maintain satisfactory levels of Cdc26 in a *gog* mutant. The retinal progenitor, in contrast, will attempt to undergo multiple amplifying divisions, quickly depleting the levels of Cdc26 equally in all of its progeny. Therefore, all retinal progenitors will arrest in mitosis and apoptose, contributing no differentiated cells to the retina in *gog* mutants.

The first potential hypothesis follows our original model where *kes* gene function normally allows a stem cell to give rise to both the retina and RPE. Division of the stem cell is biased towards forming RPE progenitors when *kes* function is lost. The increased numbers of RPE progenitors divide conservatively and maintain sufficient levels of Cdc26 in a *gog-kes* double mutant. The increase in peripheral RPE is due to the increased number of RPE progenitors. This expansion is minimally affected by the loss of Cdc26 because the RPE progenitors are more resistant since they do not dilute their store. The

CMZ is reduced because there are fewer retinal progenitors (due to *kes*) and also because the retinal progenitors arrest in mitosis and die (due to *gog*).

We did not analyze *gog-kes* double mutants at a late larval stage to rigorously determine whether the expansion of the peripheral RPE was similar in extent to a *kes* single mutant. At 5 dpf, the expansion of the peripheral RPE is grossly similar in *kes* mutants and *gog-kes* double mutants as described in Chapter 1. We predict that the expansion of the peripheral RPE would be less extensive in *gog-kes* double mutants than *kes* mutants at late larval stages, such as 9 dpf. This would suggest that RPE progenitors are eventually unable to maintain sufficient levels of Cdc26 and arrest in mitosis and die.

The second potential hypothesis is that *kes* has an essential function, similar to Cdc26, although the function of *kes* may not be related to the cell cycle. In this case, *kes* is a stronger mutation because cells run out of *kes* before they run out of Cdc26. This could be due to fewer original maternal stores, higher concentration required fo functionality, or lower stability of the *kes* protein. In this case, the observed expansion in the RPE is due exclusively to the resistance of RPE progenitors to loss of *kes*. In *gog-kes* double mutants, the peripheral RPE continues to grow while the neural retina does not, thus resulting in an expanded RPE. If this is true, *kes* mutants and *gog-kes* double mutants will have the same extent of expanded RPE at all stages. If *kes* and Cdc26 have similarly essential functions, then the *kes* mutant phenotype neither supports nor disproves the existence of a stem cell that can give rise to both RPE and neural retina.

The third possible explanation relies on *kes* regulating the cell cycle or cytokinesis, but is again more severe or has an earlier phenotypic onset. We hypothesize that RPE progenitors respond differently than retinal progenitors to a mitotic arrest and

that RPE progenitors are able to maintain a prolonged mitosis without dying. If this is the case, each stem cell division gives rise to RPE progenitors that accumulate at the periphery and cannot differentiate in *kes* mutants. These RPE progenitors are likely to have an altered morphology. In contrast, each stem cell division that gives rise to retinal progenitors will result in cells that eventually die, contributing no new cells to the neural retina in *kes* mutants. The phenotype of the *gog-kes* double mutant will not dramatically differ from a *kes* mutant, because they both result in a mitotic arrest. If this is the case, *gog* mutants should also have abnormally shaped or abnormal numbers of peripheral RPE cells. Indeed, both *vij* and *gog* have a slightly swollen peripheral RPE in comparison to wild-type, although it is not nearly as dramatic as *kes* and *oui.* Additionally, in marginal zone mutants from the insertional collection, the genes regulating replication (i.e. MCM2, MCM3, RFC4, RFC5, and DMAP1) also have an enlarged or dysmorphic RPE at some position along the peripheral edge of the retina (Gross et al., 2005).

These models will be best distinguished when the identity of the *kes* gene is revealed. Stavit Biton, a postdoctoral researcher in Vince Tropepe's group at the University of Toronto, has taken over the effort to positionally clone this mutant (as well as the Class II mutant, *rys*). Her findings will help to clarify the relationship between Cdc26 and *kes*. Thus far, our knowledge of how stem cells are regulated is fragmentary. The identity of *kes* (as well as the other 15 uncloned mutants) will enrich our understanding of the mechanisms used by post-embryonic stem cells to self-renew and maintain pluripotency.

REFERENCES

Cheng, T., Rodrigues, N., Shen, H., Yang, Y., Dombkowski, D., Sykes, M., and Scadden, D. T. (2000). Hematopoietic stem cell quiescence maintained by p21cip1/waf1. Science *287*, 1804-1808.

Eckfeldt, C. E., Mendenhall, E. M., and Verfaillie, C. M. (2005). The molecular repertoire of the 'almighty' stem cell. Nat Rev Mol Cell Biol *6*, 726-737.

Fortunel, N. O., Otu, H. H., Ng, H. H., Chen, J., Mu, X., Chevassut, T., Li, X., Joseph, M., Bailey, C., Hatzfeld, J. A., *et al.* (2003). Comment on " 'Stemness': transcriptional profiling of embryonic and adult stem cells" and "a stem cell molecular signature". Science *302*, 393; author reply 393.

Gross, J. M., Perkins, B. D., Amsterdam, A., Egana, A., Darland, T., Matsui, J. I., Sciascia, S., Hopkins, N., and Dowling, J. E. (2005). Identification of zebrafish insertional mutants with defects in visual system development and function. Genetics *170*, 245-261.

Harrison, D. A., McCoon, P. E., Binari, R., Gilman, M., and Perrimon, N. (1998). Drosophila unpaired encodes a secreted protein that activates the JAK signaling pathway. Genes Dev *12*, 3252-3263.

Hou, S. X., Zheng, Z., Chen, X., and Perrimon, N. (2002). The Jak/STAT pathway in model organisms: emerging roles in cell movement. Dev Cell *3*, 765-778.

Ivanova, N. B., Dimos, J. T., Schaniel, C., Hackney, J. A., Moore, K. A., and Lemischka, I. R. (2002). A stem cell molecular signature. Science *298*, 601-604.

Kiger, A. A., Jones, D. L., Schulz, C., Rogers, M. B., and Fuller, M. T. (2001). Stem cell self-renewal specified by JAK-STAT activation in response to a support cell cue. Science *294*, 2542-2545.

Lessard, J., Baban, S., and Sauvageau, G. (1998). Stage-specific expression of polycomb group genes in human bone marrow cells. Blood *91*, 1216-1224.

Ramalho-Santos, M., Yoon, S., Matsuzaki, Y., Mulligan, R. C., and Melton, D. A. (2002). "Stemness": transcriptional profiling of embryonic and adult stem cells. Science *298*, 597-600.

Tulina, N., and Matunis, E. (2001). Control of stem cell self-renewal in Drosophila spermatogenesis by JAK-STAT signaling. Science *294*, 2546-2549.

Yamashita, Y. M., Fuller, M. T., and Jones, D. L. (2005). Signaling in stem cell niches: lessons from the Drosophila germline. J Cell Sci *118*, 665-672.

Yamashita, Y. M., Jones, D. L., and Fuller, M. T. (2003). Orientation of asymmetric stem cell division by the APC tumor suppressor and centrosome. Science *301*, 1547-1550.

Zeidler, M. P., Bach, E. A., and Perrimon, N. (2000). The roles of the Drosophila JAK/STAT pathway. Oncogene *19*, 2598-2606.